AFRL-VS-HA-TR-98-0028

BROADBAND SEISMIC CHARACTERIZATION OF THE ARABIAN SHIELD

J. E. Zollweg and Dean M. Childs

Boise State University
Department of Geosciences
Boise, ID 83725

February 1998

Final Report
for period 8/14/95 to 1/31/98

Approved for public release; distribution unlimited

19990105 113

DEPARTMENT OF ENERGY
Office of Non-Proliferation
and National Security
Washington, DC 20585

AIR FORCE RESEARCH LABORATORY
Space Vehicles Directorate
29 Randolph Road
AIR FORCE MATERIEL COMMAND
HANSCOM AFB, MA 01731-3010

Reproduced From
Best Available Copy

SPONSORED BY
Department of Energy
Office of Non-Proliferation and National Security

MONITORED BY
Air Force Research Laboratory
CONTRACT No. F19628-95-K-0018

The views and conclusions contained in this document are those of the authors and should not be interpreted as representing the official policies, either express or implied, of the Air Force or U.S. Government.

This technical report has been reviewed and is approved for publication.

JAMES C. BATTIS
Contract Manager

CHARLES P. PIKE, Deputy Director
Integration and Operations Division

This report has been reviewed by the ESD Public Affairs Office (PA) and is releasable to the National Technical Information Service (NTIS).

Qualified requestors may obtain copies from the Defense Technical Information Center. All others should apply to the National Technical Information Service.

If your address has changed, or you wish to be removed from the mailing list, or if the addressee is no longer employed by your organization, please notify AFRL/VSOS-IM, 29 Randolph Road, Hanscom AFB, MA 01731-3010. This will assist us in maintaining a current mailing list.

Do not return copies of the report unless contractual obligations or notices on a specific document requires that it be returned.

REPORT DOCUMENTATION PAGE

Form Approved
OMB No. 0704-0188

Public reporting burden for this collection of information is estimated to average 1 hour per response, including the time for reviewing instructions, searching existing data sources, gathering and maintaining the data needed, and completing and reviewing the collection of information. Send comments regarding this burden estimate or any other aspect of this collection of information, including suggestions for reducing this burden, to Washington Headquarters Services, Directorate for Information Operations and Reports, 1215 Jefferson Davis Highway, Suite 1204, Arlington, VA 22202-4302, and to the Office of Management and Budget, Paperwork Reduction Project (0704-0188), Washington, DC 20503.

1. AGENCY USE ONLY *(Leave blank)*	2. REPORT DATE	3. REPORT TYPE AND DATES COVERED
	February 1998	Final 8/14/95 - 1/31/98

4. TITLE AND SUBTITLE

Broadband Seismic Characterization of the Arabian Shield

5. FUNDING NUMBERS

C F19628-95-K-0018
PE 69120H
PR DENN
TA GM
WU AG

6. AUTHOR(S)

J. E. Zollweg and D. M. Childs

7. PERFORMING ORGANIZATION NAME(S) AND ADDRESS(ES)

Department of Geosciences
Boise State University
Boise, ID 83725

8. PERFORMING ORGANIZATION REPORT NUMBER

9. SPONSORING / MONITORING AGENCY NAME(S) AND ADDRESS(ES)

Air Force Research Laboratory
29 Randolph Road
Hanscom AFB, MA 01731-3010
Contract Manager: James Battis/VSBI

10. SPONSORING / MONITORING AGENCY REPORT NUMBER

AFRL-VS-HA-98-0028

11. SUPPLEMENTARY NOTES

This research was sponsored by the Department of Energy, Office of Non-Proliferation and National Security, Washington, DC 20585

12a. DISTRIBUTION / AVAILABILITY STATEMENT

Approved for public release; distribution unlimited

12b. DISTRIBUTION CODE

13. ABSTRACT *(Maximum 200 words)*

Seismograms recorded on broadband instruments in Saudi Arabia for events occurring in the Zagros Folded Belt of Iran often show a *P* phase with an apparent velocity of about 5.7 km/sec. We refer to this phase as P_x. Its amplitude rapidly diminishes along Arabian Shield paths, suggesting it is a guided wave in the sedimentary section of the Arabian Platform. P_x blockage is observed for event-station paths crossing the Zagros and for some other events that we believe occur below the wave guide. Both the amplitude variation observed for P_x and its probable nature as a relatively slow guided wave in the upper crust suggest that the phase has potential for use in focal depth determination by regional stations.

14. SUBJECT TERMS	15. NUMBER OF PAGES
Arabian Shield, Arabian Platform, regional seismic phases, focal depths	52
	16. PRICE CODE

17. SECURITY CLASSIFICATION OF REPORT	18. SECURITY CLASSIFICATION OF THIS PAGE	19. SECURITY CLASSIFICATION OF ABSTRACT	20. LIMITATION OF ABSTRACT
Unclassified	Unclassified	Unclassified	UL

DTIC QUALITY INSPECTED 8

CONTENTS

DTIC QUALITY INSPECTED 5

Deployment of Broadband Seismographs in Saudi Arabia

Broadband seismographs were deployed at nine sites in Saudi Arabia between late 1995 and early 1997. The deployment was a joint project of the University of California at San Diego (UCSD), King Saud University (KSU), King Abdul Aziz City of Science and Technology (KACST), and Boise State University (BSU). BSU made the initial contacts that were necessary for Saudi approval of the project and was responsible for vault construction. UCSD selected and installed the sites and was responsible for data management. KSU and KACST provided logistical support and part of the routine data recovery. As many as seven recording sites operated concurrently. The objective of the study was characterization of recording sites and seismic wave propagation in the Arabian Shield, a large granitic terrain that is mainly exposed in western Saudi Arabia (Figure 1). All but one of the sites occupied were placed on shield rocks. The remaining site (RIYD) was operated on sedimentary rocks of the Arabian Platform, which bounds the Arabian Shield on the east. All sites utilized STS-2 broadband three-component seismometers, whose output was sampled at 40 Hz and recorded continuously on-site on Reftek digital data acquisition systems. Timing was provided by internal clocks slaved to GPS receivers. Data were periodically recovered by personnel of KSU and/or UCSD, and were processed by UCSD. The data archive has been made publicly available through the Data Management Center of the Incorporated Research Institutions in Seismology.

Locations of the nine stations operated in Saudi Arabia are given in Table 1. The initial deployment included a site near the eastern edge of the Arabian Shield at Ar Rayn (RAYN). This site was converted to a Global Digital Seismic Network (GDSN) station in June, 1996. The GDSN station has operated continuously to the present.

The recorded data set provides a unique glimpse of seismicity and seismic wave propagation in an area that previously had been little studied. The sites were found to have very low levels of high frequency background noise, making them some of the best short-period recording sites in the world. The high historical seismicity levels (Figure 2) that prevail around the Arabian Peninsula insured that a variety of path and source conditions would be sampled by the recorded

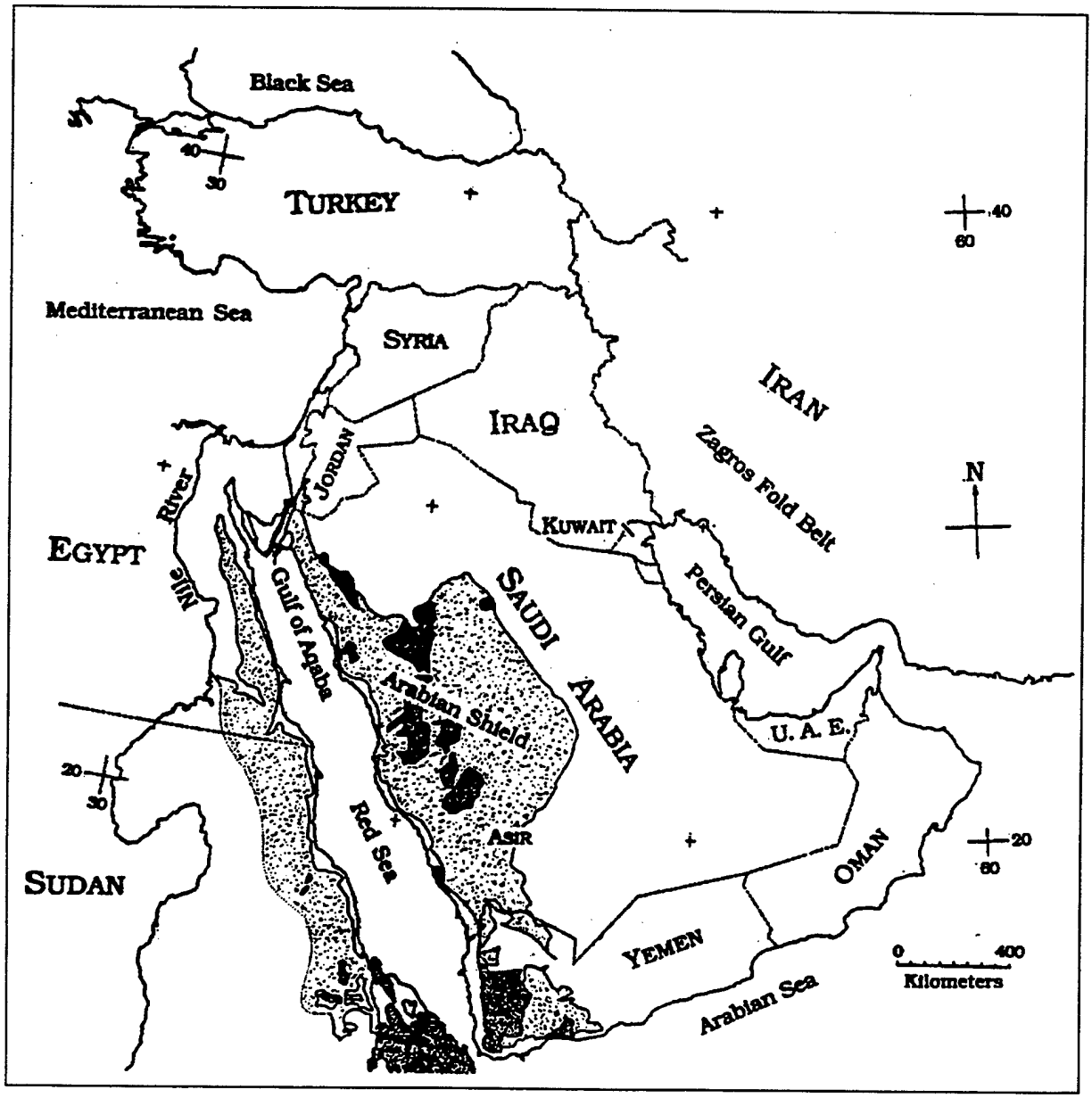

Figure 1. The Arabian Peninsula region, showing the location of the Arabian Shield (lightly stippled region). Dark stippled areas show where Cenozoic basalts overlie the shield rocks.

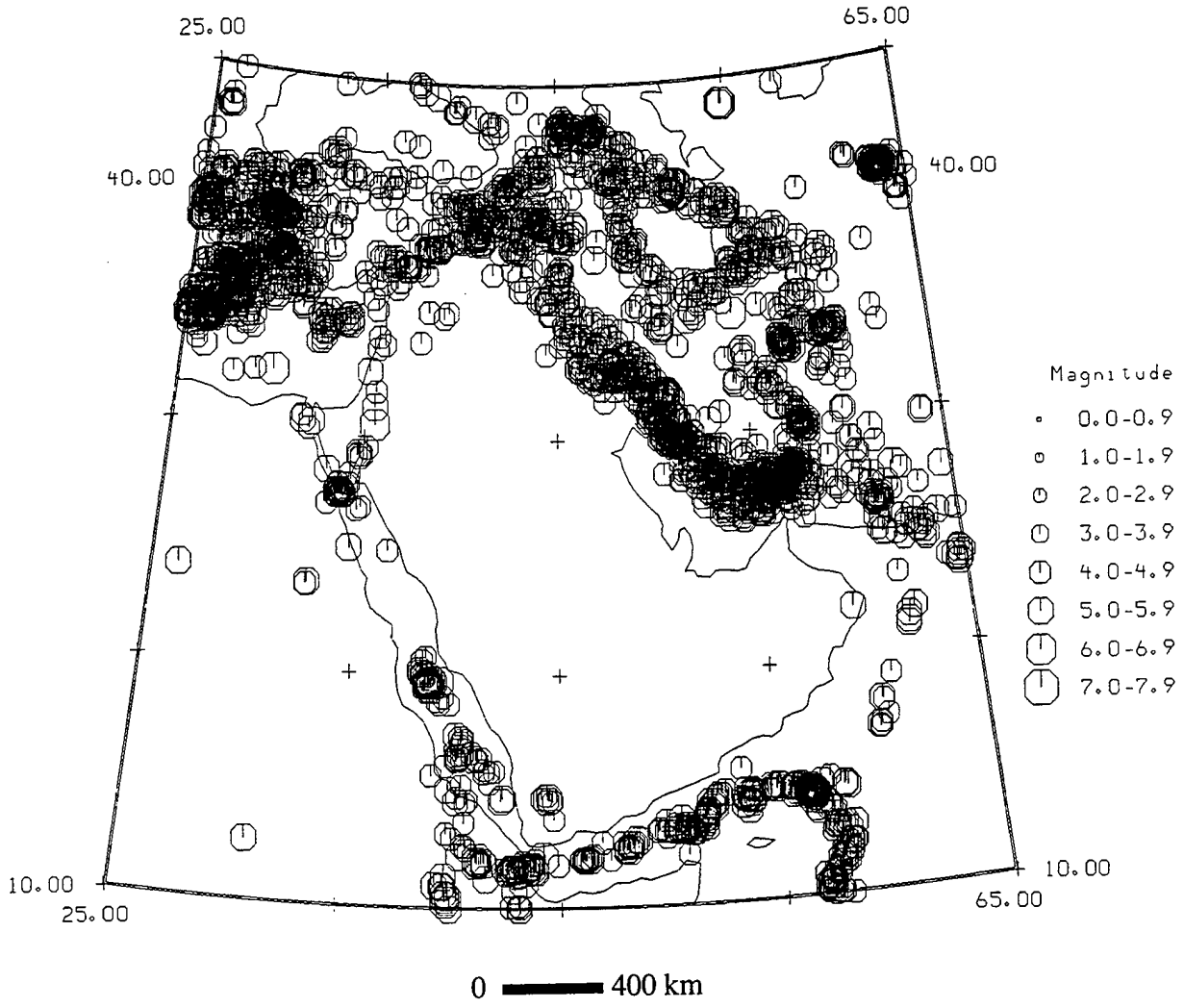

Figure 2. Seismicity of the Arabian Peninsula region, taken from the NOAA data base. Map shows events of magnitude 4.5 or greater occurring through mid-1988.

TABLE 1: BROADBAND STATION SITES

Code	N Latitude dg mn sec	E Longitude dg mn sec	Elevation km	Site
AFIF	23 55 51.60	43 02 24.00	1.116	Afif
BISH	19 55 22.10	42 41 24.40	1.379	Bisha
HALM	22 50 43.40	44 19 02.30	0.930	Hadabat Al-Mahri
RANI	21 18 41.80	42 46 34.00	1.001	Raniyah
RAYN	23 31 19.20	45 30 02.90	0.792	Ar-Rayn
RIYD	24 43 19.20	46 38 34.80	0.717	Riyadh
SODA	18 17 31.60	42 22 36.80	2.876	Al-Soda
TAIF	21 16 51.60	40 20 56.40	2.050	Taif
UQSK	25 47 20.40	42 21 36.00	0.950	Uqlat As Suqur

events, and such was indeed the case. Some details of detection capabilities have been given by Vernon *et al.* (1996).

Zagros Folded Belt Seismicity

The area of highest persistent seismicity closest to the Arabian Peninsula is the Zagros Folded Belt of western Iran (see Figures 1 and 2). Sporadic high seismicity occurs in the Gulf of Aqaba near the Saudi Arabian - Jordanian - Israeli boundary, including a magnitude 7.2 event just a few hours prior to the installation of the first station for this study. This source zone is relatively limited spatially and does not have the tectonic or political implications that characterize some other regional seismic sources close to Saudi Arabia. We chose to study some of the recorded characteristics of events in the Zagros region, which is of interest for monitoring compliance with the Comprehensive Nuclear Test Ban Treaty (CTBT). Figure 3 shows the events in the Zagros Folded Belt region that were reported by the U. S. Geological Survey's Preliminary Determination of Epicenters program (PDE) during the broadband deployment.

The Zagros Mountains and fold belt are the result of continental collision between the Arabian and Persian plates (Jackson and Fitch, 1981). Events with subcrustal focal depths have been reported beneath the Zagros Mountains, a point to which we shall return later. Most of the recorded seismicity is believed to occur within the rocks of the Arabian Plate. This latter factor is important because it indicates that most of the event-station paths that will be observed for recording sites in the Arabian Peninsula are relatively simple ones through the Arabian Plate.

While extensive geophysical studies have been performed in the Persian Gulf area due to petroleum exploration, we do not know of any regional-scale crustal refraction studies that traverse the entire region from the Zagros to the Arabian Shield. Mooney *et al.* (1985) performed a refraction experiment running from the Riyadh region (on the Arabian Platform) to the Red Sea. Their first-order model of the Arabian shield consists of two layers, each 20 km thick, characterized by P velocities of 6.3 and 7.0 km/sec. The depth to the Moho averages about 40 km, and the upper mantle P_n velocity is 8.0 - 8.2 km/sec. While the lack of knowledge

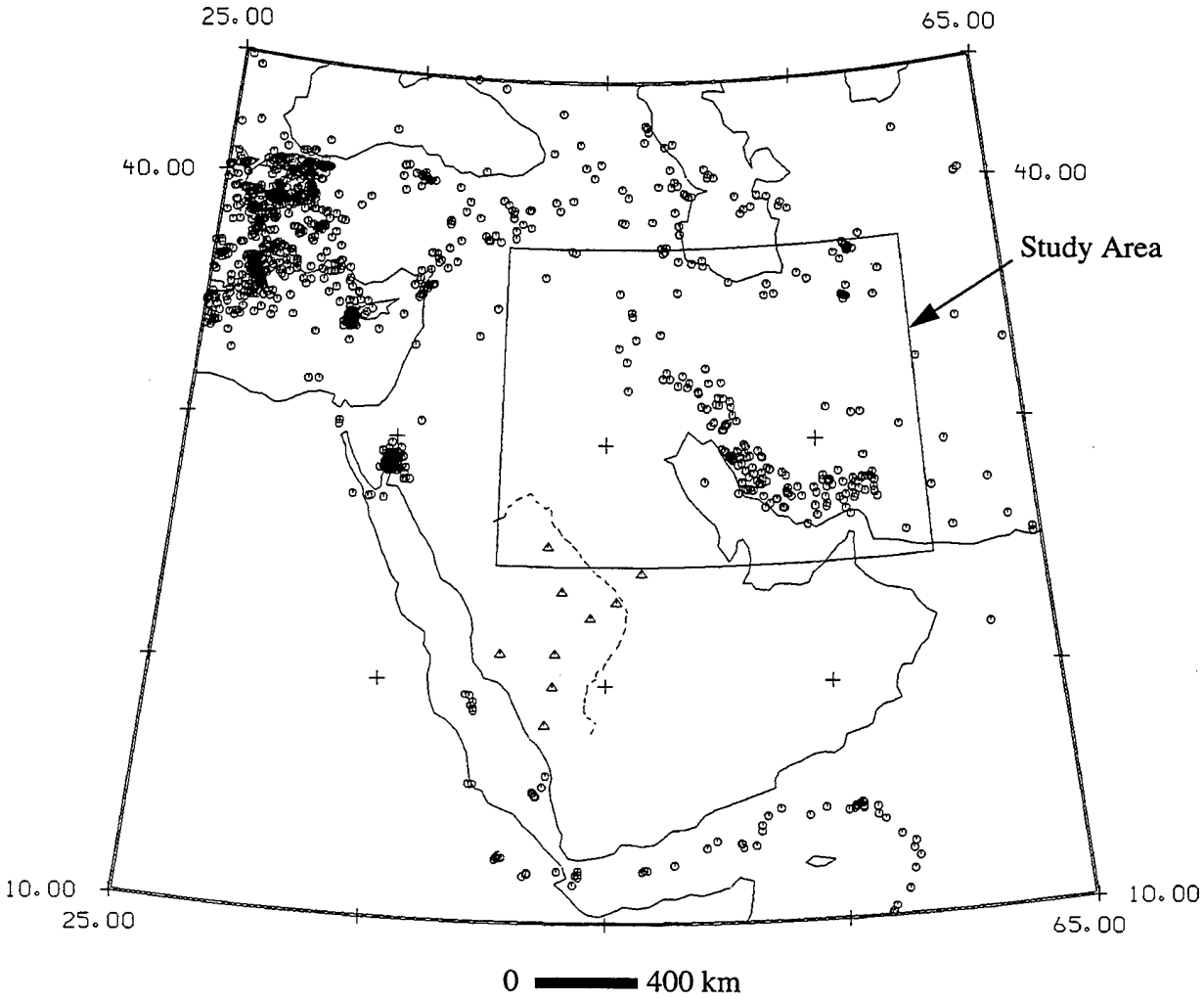

Figure 3. Epicenters reported by PDE during the Arabian Shield broadband deployment, November 1995 - February 1997. Locations of broadband stations are shown as triangles. Dashes show the eastern limit of the Arabian Shield.

of details of crustal structure to the east of the Arabian Shield is a drawback, it is still possible to draw a conceptual model of structure between the Shield and the Zagros, since the Arabian Platform is generally believed to be a relatively undeformed domain of nearly flat-lying shallow marine sedimentary formations. Mooney *et al.* interpreted the boundary between the eastern Arabian Shield and the Arabian Platform as a suture zone between crustal blocks of differing composition. If this interpretation is correct, there could be some disruption of the crustal wave guide for Zagros events despite their intra-Arabian Plate paths.

Characteristics of Seismograms of Zagros Region Events as Recorded by Arabian Shield Stations

Our interest in examining Saudi broadband seismograms was to see what kinds of secondary *P* phases were recorded, since these phases may be useful in making independent focal depth determinations. Our initial data set was all events located by PDE within the area 18 - 39° N, 40 - 61° E, during the Saudi broadband deployment. This region (see Figure 1) covers much of the Arabian Peninsula and most of Iran and Iraq, as well as small portions of other countries. Excerpts of the continuous data streams were made for each operating broadband station. We windowed time segments for the events shown in Figure 3 from the continuous time series, running from one minute prior to the expected *P* arrival to a group velocity of 3.3 km/sec. We expected that such windows would encompass all crustal phases of interest from P_n to the L_g phase. Actually, what appears to be L_g on the seismograms has a somewhat lower apparent velocity, about 3.2 km/sec, than normal. On the seismograms shown in this report we will emphasize this point by denoting the apparent L_g arrival as "L_g". Seismograms were high-pass filtered with a corner at 0.5 Hz to suppress low-frequency microseismic noise. Because of the small magnitude of most of the events and occasional operational problems, it was rare that all operating stations recorded a particular event. Events found to have very low signal/noise ratios in the *P*-wave portion of the seismograms were not analyzed.

P_n and S_n Phases

P_n and S_n were observed to be clear phases with distinct, easily-identified onsets, as might be expected from the shield environment and intraplate paths. Figure 4, a fairly typical three-component set of records from the Ar Rayn (RAYN) station, shows the identified P_n and S_n arrivals for the event of 0148 UTC on 8 March 1996. It is relatively rare for seismograms from the Arabian Shield stations to show much complication, implying that a good waveguide exists at the base of the crust. Instead, the simplicity of the seismograms is what seems more remarkable. With the exception of the phase (denoted as P_x in Figure 4) that will be the main point of discussion in this report, there is little evidence of the many arrivals that make up the complicated seismograms observed in most regions of crustal seismicity. The clean recording characteristics observed for P_n and S_n imply that the Arabian Shield is an excellent place to monitor regional seismicity. The lack of other observed phases is somewhat puzzling, given the interpreted layered structure and the large velocity contrasts between layers. Some possible explanations will be postulated later in this report.

P_x -- A Prominent Secondary P Phase Observed for Many Zagros Fold Belt Events

A prominent characteristic of many of the observed seismograms is a relatively large and impulsive phase arriving between P_n and S_n (often somewhat closer to S_n) that we have termed P_x. This phase arrives too late to be P_g, assuming the usual P_g velocity of about 6.1 km/sec or the Arabian Shield upper layer velocity of 6.3 km/sec. On most seismograms, no phase is identifiable that might correspond to P_g with a more typical velocity. We will return to the issue of nomenclature in the discussion section at the end of this report.

Figure 5 shows the events in the Zagros Folded Belt region that we found to have an adequate signal/noise ratio for the examination of P phases following the initial P_n arrival. We only plotted those events whose data were used in our analysis of phases, which is mainly equivalent to applying a low magnitude cut-off and does not distort the overall seismicity pattern. Table

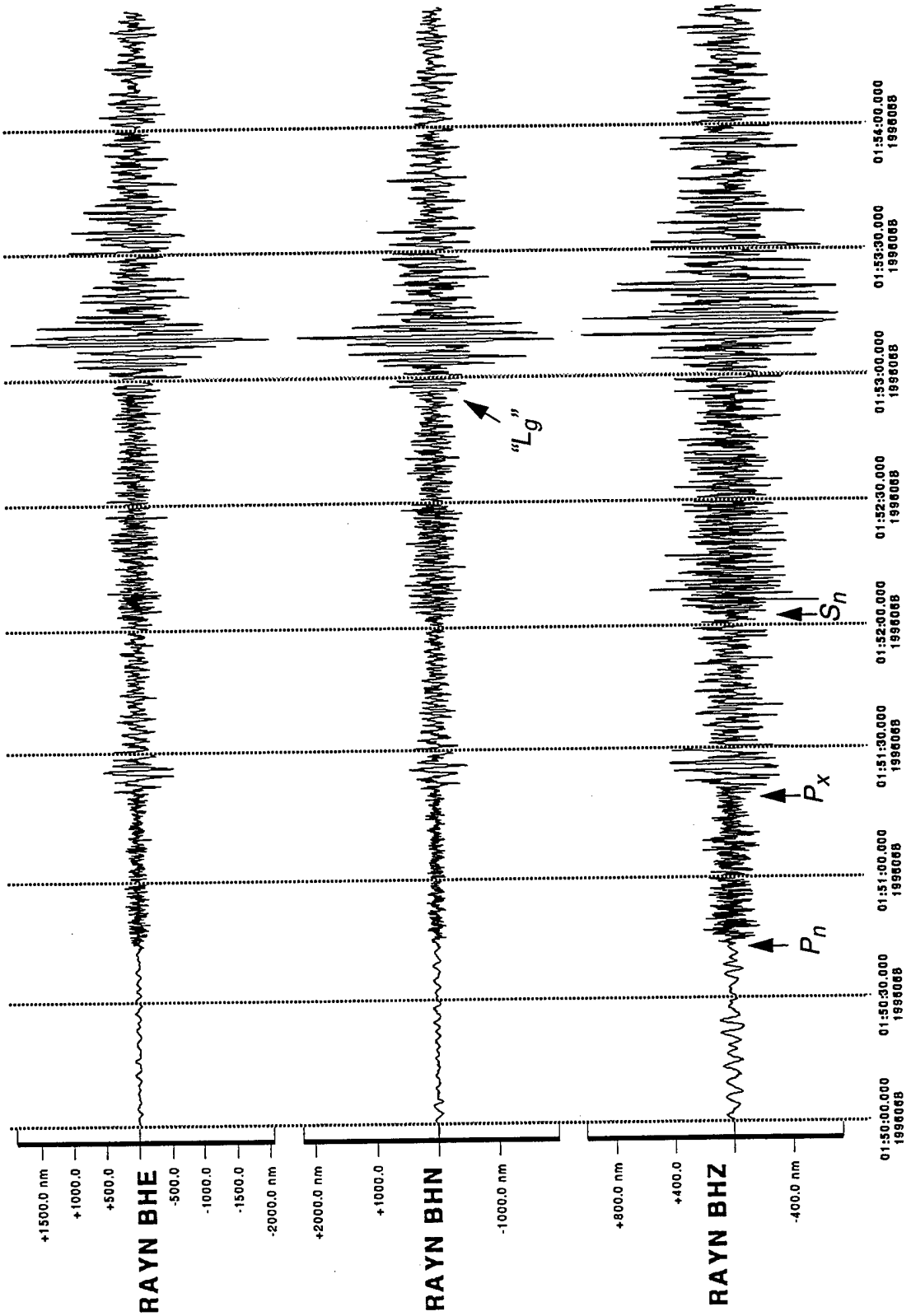

Figure 4. P_n, S_n, and P_x as recorded at Ar Rayn (RAYN) for the event of 01:48 UTC, 08 March 1996.

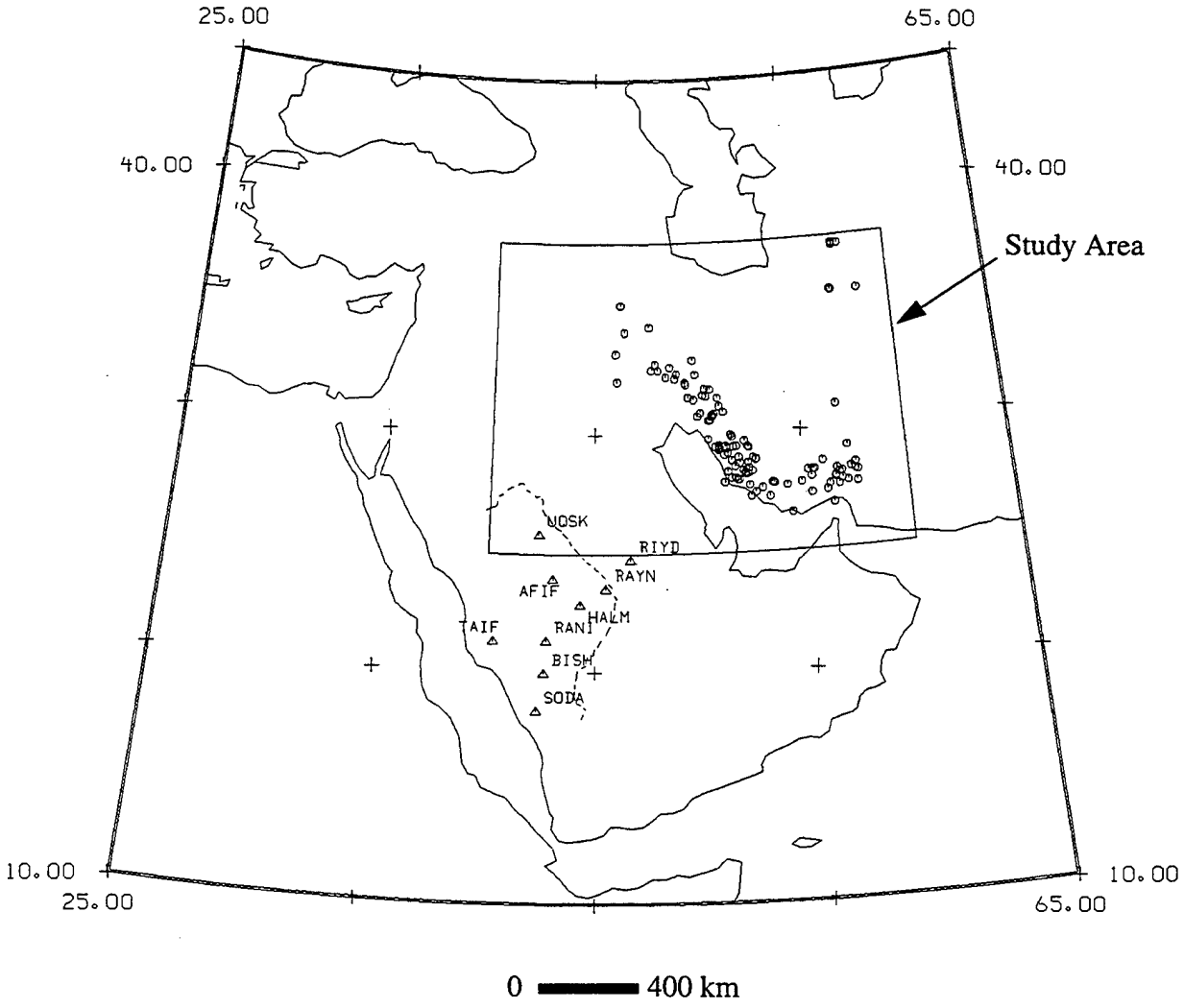

Figure 5. PDE epicenters of events analyzed in this study.

2 gives the pertinent hypocentral information.

The strength and character of the P_x phase varied significantly from event to event and from station to station for the same event. When recorded, this phase is notable because of the general lack of any other apparent phase arrival between P_n and S_n. P_x does not correspond to the "standard" crustal phases P^* or P_g, nor does it appear to be a reflection like P_mP. All of these phases should arrive closer in time to P_n. We believe P_x is a guided wave through upper crustal sedimentary rocks of the Arabian Platform. While such a phase may be considered analogous to P_g, we believe the velocity difference and some of the attenuation characteristics observed for P_x make a distinction useful, since true P_g phases may be observed for other paths in the Arabian Shield having more typical velocity structure.

Examples of some typical seismograms of observed P_x are shown in Figure 6. P_x is generally a very noticeable phase, and because it has an overall lower frequency content than the P_n coda it is often observable at SNR less than one. In fact, it was often difficult to say that P_x was NOT recorded on a particular station. Another characteristic of P_x is that it is usually more strongly recorded on the radial horizontal component than on the vertical. Based upon a limited number of amplitude observations (32, mostly made for events in the early part of the deployment), the larger horizontal component is an average of 1.2 times larger than the vertical component.

To analyze this phase, a simple subjective scheme of "strong","weak", "not present" or "not classifiable" was initially adopted. The subjective classification was compared to signal/noise ratio (SNR) thresholds, where the signal amplitude is taken as the maximum trace amplitude of P_x as observed on broadband vertical component seismograms high-pass filtered at 0.5 Hz, and the noise amplitude was the trace amplitude of the P wave coda in the few seconds (usually 20 or more) preceding the first arrival of P_x. It should be noted that these measurements are themselves somewhat subjective, particularly the measurement of the noise amplitude. The SNR ratios ranged from less than unity to greater than ten; the range of observed SNR ratios is shown in Figure 7. Based upon the peaks in the "weak" and "strong" distributions, we found that

TABLE 2
PDE LOCATIONS FOR EVENTS ANALYZED

YEAR	MO	DA	TIME	N LAT	E LONG	DEPTH		MB
1995	11	24	224442.49	32.319	48.942	73	*	4.5
1995	11	27	143229.07	32.308	48.923	61		5.0
1995	12	04	193536.14	27.833	54.883	33	N	4.8
1995	12	18	034511.09	30.558	50.644	33	N	4.6
1995	12	20	020921.43	28.607	51.765	33	N	4.5
1995	12	21	073900.25*	27.751	57.145	33	N	4.1
1995	12	24	135411.59*	27.367	55.351	33	N	4.1
1995	12	24	150648.15	32.377	48.483	33	N	4.5
1995	12	28	182335.09	27.948	56.552	46	*	4.6
1995	12	28	202748.35*	27.997	56.565	86	?	4.1
1995	12	31	105300.92*	29.422	52.383	33	N	4.3
1995	12	31	115639.55	29.385	52.442	33	N	4.7
1996	01	03	084225.75	38.994	48.720	56		4.9
1996	01	04	103141.73	32.130	49.435	33	N	4.8
1996	01	06	103148.80	29.687	51.233	33	N	4.4
1996	01	12	102318.13*	28.529	52.419	33	N	4.0
1996	01	13	095717.64	28.326	57.325	33	N	4.3
1996	01	24	052807.41	29.500	51.020	44	*	4.5
1996	01	24	060526.03	29.356	51.008	34	D	4.4
1996	01	24	070704.74	29.414	51.033	57	*	4.7
1996	01	25	180521.51	29.299	51.006	48	*	4.5
1996	01	25	204355.26*	32.202	46.057	10	G	4.5
1996	01	26	131113.85	29.343	51.008	33	N	4.6
1996	01	26	170216.58	29.331	51.032	33	N	4.4
1996	01	26	190128.73	28.749	52.379	33	N	4.4
1996	01	28	084316.36	34.270	46.459	33	N	4.9
1996	01	31	204334.01	31.861	50.393	65	*	4.6
1996	02	05	082813.78	35.671	58.395	33	N	4.8
1996	02	16	025053.38?	26.892	56.387	33	N	4.1
1996	02	16	214004.80	31.127	51.082	33	N	4.3
1996	02	25	161411.64	35.725	56.990	33	N	4.8
1996	02	25	174204.66	35.685	57.038	33	N	4.9
1996	03	03	084536.32?	27.508	52.700	33	N	3.8
1996	03	04	013530.32	27.663	56.253	33	N	4.5
1996	03	07	032814.11?	28.312	55.223	33	N	3.8
1996	03	08	014856.29*	28.061	51.950	33	N	4.1
1996	03	13	080530.01?	28.869	51.611	33	N	4.0
1996	03	16	023143.52*	28.291	56.631	33	N	4.0
1996	03	16	032451.84?	29.174	51.432	33	N	4.0
1996	03	16	201833.05*	29.315	51.027	33	N	4.3
1996	03	18	031142.71*	29.476	51.012	33	N	4.0
1996	03	20	015453.76?	28.399	51.413	41	D	3.9
1996	03	20	222404.48	29.474	50.992	33	N	4.5
1996	03	23	040211.37	28.880	52.766	33	N	4.3
1996	03	27	033347.75*	28.742	51.999	33	N	4.0
1996	03	31	150724.51?	29.444	50.835	33	N	3.7
1996	03	31	160206.07	32.051	49.468	33	N	4.3
1996	03	31	211328.20*	29.774	50.515	36	?	4.1
1996	04	02	104124.48*	29.427	51.705	33	N	3.9

TABLE 2 (CONTINUED)
PDE LOCATIONS FOR EVENTS ANALYZED

YEAR	MO	DA	TIME	N LAT	E LONG	DEPTH		MB
1996	04	09	173823.61*	28.168	56.863	33	N	4.0
1996	04	10	202607.84	28.874	52.736	33	N	4.2
1996	04	11	200012.24*	32.494	49.025	33	N	3.8
1996	04	15	141042.58*	26.593	54.382	33	N	4.0
1996	04	18	201304.50*	27.865	56.868	33	N	4.0
1996	04	20	183028.23	28.056	51.874	33	N	4.0
1996	05	01	224209.16%	28.394	52.574	33	N	3.9
1996	05	03	073642.50*	29.210	57.208	33	N	4.2
1996	05	06	101811.02%	32.792	48.698	33	N	3.8
1996	05	10	152300.39	30.862	50.166	33	N	4.3
1996	05	18	201022.74*	34.479	47.684	33	N	3.8
1996	05	24	063558.79	27.847	53.594	33	N	4.9
1996	05	25	170057.53	27.886	53.521	33	N	4.7
1996	05	29	092406.06*	28.131	51.593	33	N	4.2
1996	06	02	124215.44	30.811	50.827	33	N	4.8
1996	06	07	050320.70	30.759	50.717	33	N	4.7
1996	06	07	051701.72%	30.734	50.767	33	N	3.9
1996	06	18	191723.08	30.693	50.699	33	N	4.0
1996	07	01	081446.86	28.288	52.258	33	N	4.3
1996	07	15	193145.55*	33.063	49.840	33	N	4.4
1996	07	16	084046.62*	32.915	47.947	33	N	4.1
1996	07	16	164616.68	32.675	47.769	33	N	4.2
1996	07	21	111842.45*	28.301	52.355	33	N	4.6
1996	08	06	202719.63	27.676	53.012	33	N	4.8
1996	08	12	235808.28%	28.135	51.794	33	N	4.2
1996	08	24	051556.33*	31.464	51.013	33	N	4.4
1996	08	25	005308.93*	32.655	48.085	33	N	4.4
1996	09	04	203952.30*	35.396	46.263	33	N	4.4
1996	09	06	123656.20	27.809	52.417	33	N	4.5
1996	09	14	190938.60*	29.842	51.647	33	N	
1996	09	16	011331.81*	28.340	52.241	33	N	
1996	09	20	215833.10?	32.460	49.962	33	N	3.9
1996	09	25	162215.95*	27.959	51.247	10	G	4.4
1996	09	26	095524.46?	29.648	52.247	33	N	
1996	09	28	135355.89	28.481	57.555	33	N	4.8
1996	09	29	211950.23*	33.365	46.002	33	N	4.5
1996	10	04	160719.49*	29.458	51.347	33	N	3.8
1996	10	15	211043.21%	27.730	54.199	33	N	
1996	10	18	092603.62	27.695	57.573	33	N	5.4
1996	10	27	014151.26*	30.714	50.010	33	N	
1996	11	08	050518.47*	31.587	50.300	33	N	4.5
1996	11	18	115215.04	29.939	51.596	33	N	5.4
1996	11	24	123548.79?	31.542	50.446	33	N	4.4
1996	11	24	183403.85?	27.298	53.359	10	G	
1996	12	04	023934.81	27.354	52.473	33	N	4.5
1996	12	09	023314.40*	31.829	50.658	108	?	4.3
1996	12	14	194951.30	28.454	49.630	10	G	4.5
1996	12	19	232001.01%	29.406	51.030	33	N	
1996	12	20	001812.84	29.359	51.390	33	N	4.6

TABLE 2 (CONTINUED)
PDE LOCATIONS FOR EVENTS ANALYZED

YEAR	MO	DA	TIME	N LAT	E LONG	DEPTH		MB
1996	12	20	061231.48*	28.430	52.154	33	N	4.0
1996	12	20	080859.91	38.86	41.09	10		4.3
1996	12	21	033205.25?	30.530	50.558	50	G	
1996	12	21	231333.78*	27.634	56.698	25	D	4.3
1996	12	26	091725.26	30.882	51.276	33	N	4.7
1996	12	31	231741.67*	28.042	55.380	33	N	3.8
1997	01	13	022410.86?	28.653	55.955	50	G	3.5
1997	01	15	152811.33*	28.980	51.953	33	N	4.0
1997	01	18	132016.87?	29.099	51.276	33	N	
1997	01	19	190613.81*	29.446	51.836	33	N	3.6
1997	01	24	171257.58	28.226	57.529	39	D	4.5
1997	02	04	095355.73	37.564	57.295	10	G	5.3
1997	02	04	103747.14	37.661	57.291	10	G	5.9
1997	02	05	075345.62	37.629	57.594	10	G	5.2
1997	02	08	032823.04	30.947	56.791	39	D	4.7
1997	02	10	042725.38*	31.504	49.588	33	N	3.8
1997	02	11	184226.91	28.170	57.638	33	N	4.3
1997	02	12	144252.64	28.325	55.449	33	N	4.5
1997	02	12	170004.04	28.324	55.532	33	N	4.3
1997	02	15	194725.94	28.953	52.638	33	N	4.8
1997	02	17	043126.99	27.441	56.110	33	N	4.9
1997	02	17	045041.36	31.421	49.842	33	N	4.5

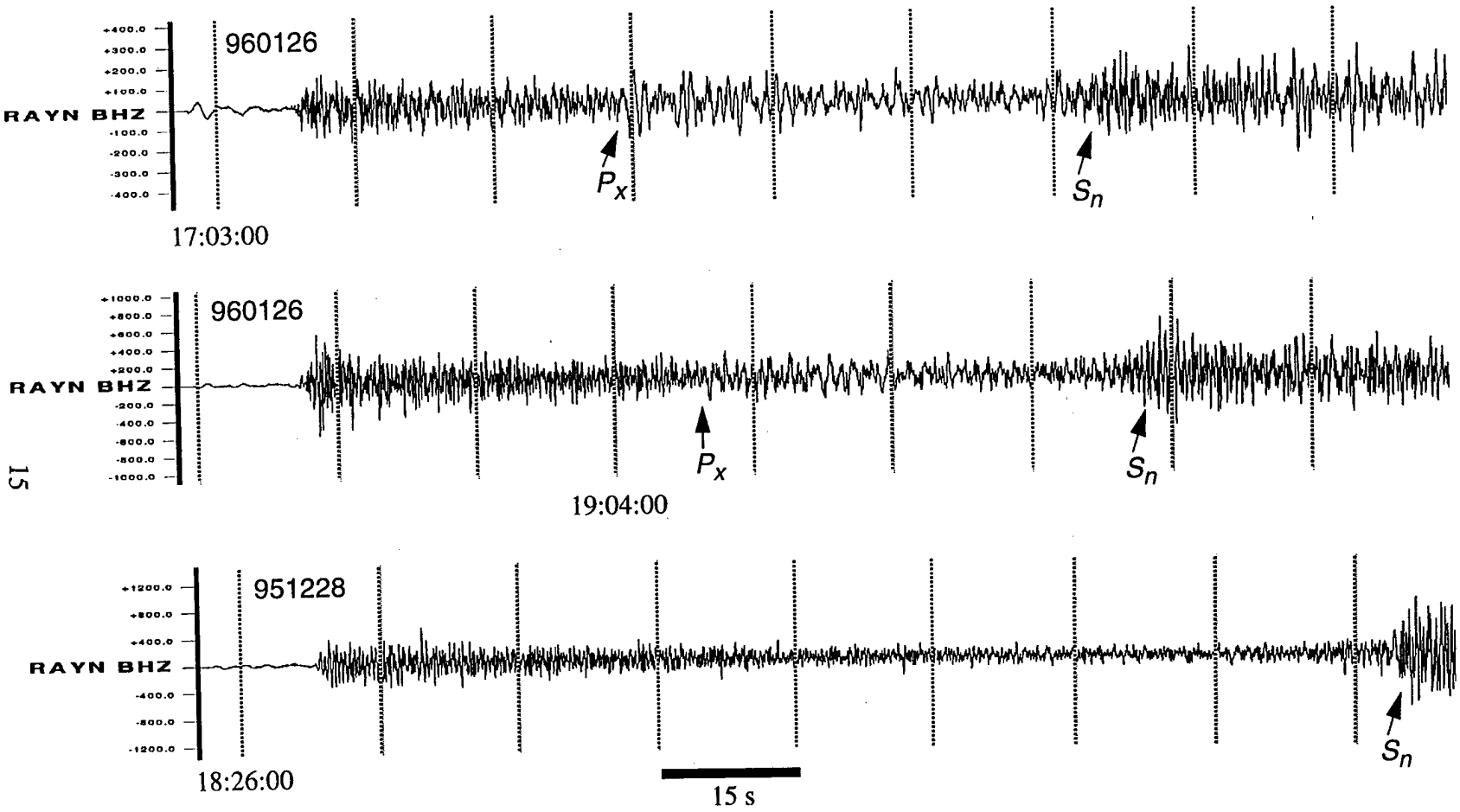

Figure 6. Some examples of P_x as recorded at Ar Rayn (RAYN). showing (from top) strong P_x, weak P_x, and P_x not present.

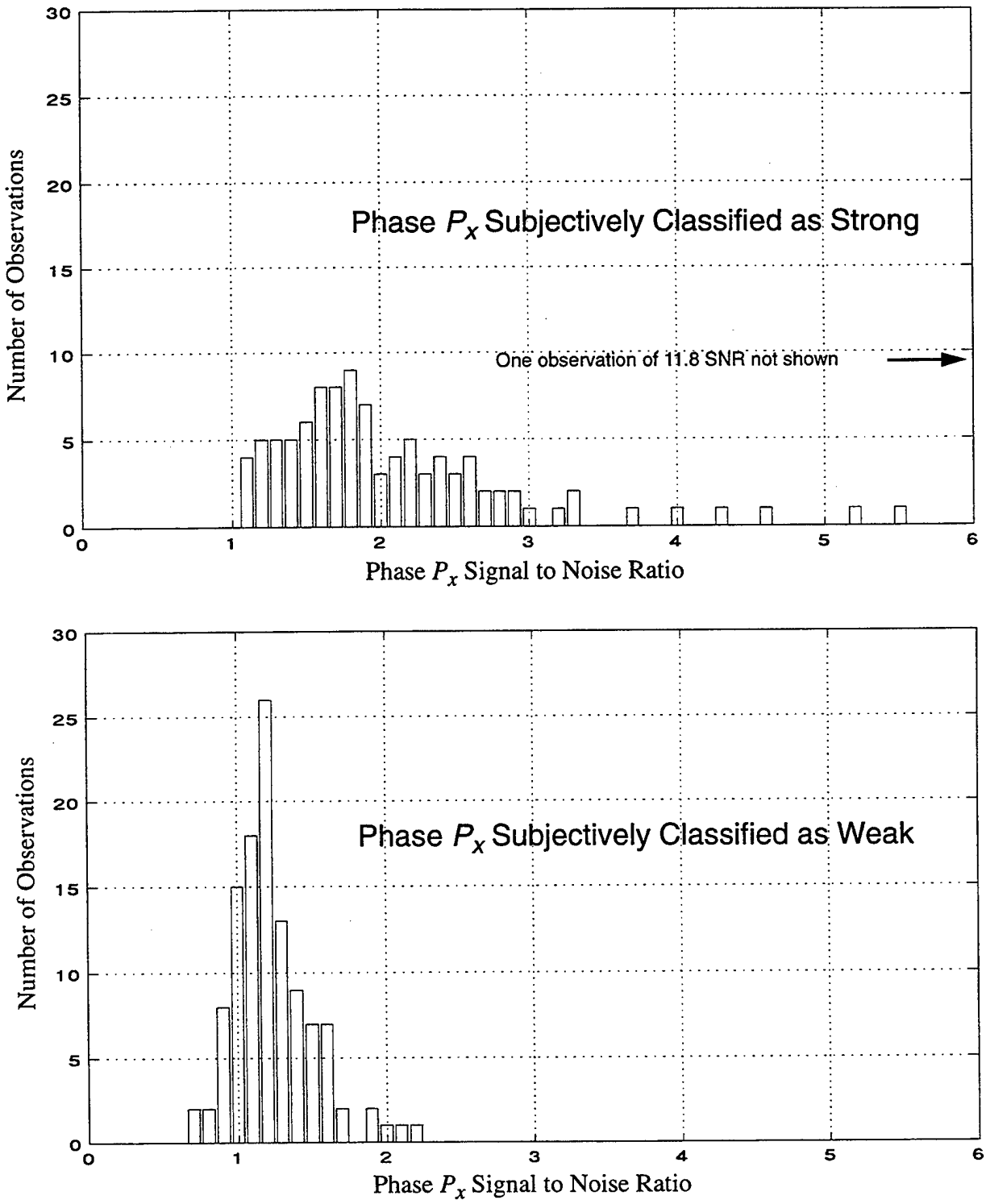

Figure 7. Signal-noise ratio (SNR) distribution of events whose P_x phase was classified as strong (top) and weak (bottom). The "noise" level was taken as being representative of the P wave coda in the several second interval preceding the apparent P_x arrival. For subsequent analysis, P_x was classified as strong if SNR exceeded 1.5. The strongest P_x observed had a SNR of 11.8.

"strong" arrivals typically had SNR greater than 1.5, while "weak" arrivals usually had SNR of 1.5 or less. We therefore set the threshold between the two classifications at SNR = 1.5. Table 3 gives our observations of P_x, including one observation for an event (1996 1220 0808Z) outside our main study area).

An example of an extremely strong recording of P_x is shown in Figure 8. The population of high SNR is arguably non-normal for SNR greater than 3 (Figure 7) and the small number of such observations were placed into a separate category (very strong). The event shown in Figure 8 is noteworthy because it clearly demonstrates that a more distant station gets little or no P_x energy, while the stations closest to the event get strong arrivals. Since the more distant stations in our study have Zagros event paths that traverse ever-increasing portions of the Arabian Shield, we believe that the poor observation of P_x at greater distances is due to either high attenuation of the phase in the shield or disruption of the wave guide, rather than simply being a function of event position (as might occur if some events were crustal and some sub-crustal). The relatively high velocities in the Arabian Shield reported by Mooney *et al.* (1985) argue that the low amplitudes in the Arabian Shield are not an attenuation effect, so we conclude that disruption of the wave guide at the Arabian Shield/Arabian Platform boundary is responsible for the poor propagation of P_x over long Arabian Shield paths.

A typical example of P_x recordings for a single event is shown in Figure 9. While the P_x phase is prominent, it is not very large. P_x often contrasts with the preceding P coda due not so much to its amplitude as its frequency content. The predominant frequency of P_x is usually much lower than that of P_n and its coda. This is interpreted as being due to either higher attenuation or a different frequency-dependent attenuation function along the path of the P_x phase.

Figure 10 shows an event for which there is no apparent P_x arrival. As noted above, it was often difficult to distinguish whether the phase does not exist on a seismogram or is simply very weakly recorded. There appears to be a continuum of recorded amplitudes down to practically vanishing. Nevertheless, there are some seismograms for which we are unable to discern any

TABLE 3.

OBSERVATIONS OF Px CHARACTER AND
SIGNAL-TO-NOISE RATIO (SNR)

DATE	UTC	STATION	CHARACTER	SNR
951124	2244	AFIF	strong	1.3
951124	2244	HALM	strong	1.1
951127	1432	AFIF	strong	1.1
951204	1935	HALM	blocked	
951204	1935	RAYN	weak	1.4
951218	0345	AFIF	strong	1.4
951218	0345	HALM	blocked	
951218	0345	RAYN	str-wk	1.2
951220	0209	HALM	strong	1.3
951220	0209	RAYN	strong	2.2
951221	0739	HALM	blocked	
951221	0739	RAYN	blocked	
951224	1354	HALM	blocked	
951224	1354	RAYN	weak	1.3
951224	1506	AFIF	weak	1.4
951224	1506	HALM	weak	1.0
951224	1506	RAYN	strong	2.3
951228	1823	AFIF	blocked	
951228	1823	HALM	blocked	
951228	1823	RAYN	blocked	
951228	2027	HALM	blocked	
951228	2027	RAYN	weak	1.1
951231	1053	AFIF	weak	0.9
951231	1053	HALM	weak	1.0
951231	1053	RAYN	strong	1.8
951231	1156	HALM	weak	1.2
951231	1156	RAYN	weak	1.2
960103	0842	HALM	blocked	
960104	1031	AFIF	strong	1.5
960104	1031	HALM	weak	
960104	1031	RANI	blocked	
960104	1031	RAYN	strong	1.8
960104	1031	SODA	blocked	
960106	1031	HALM	weak	1.2
960112	1023	HALM	weak	1.1
960112	1023	RAYN	strong	2.0
960113	0957	HALM	blocked	
960113	0957	RAYN	blocked	
960124	0528	HALM	strong	1.4
960124	0528	RAYN	strong	2.2
960124	0605	RAYN	weak	1.1
960124	0707	HALM	strong	1.7
960124	0707	RANI	weak	1.2
960124	0707	RAYN	strong	1.8
960125	1805	HALM	weak	
960125	1805	RAYN	strong	
960125	2043	HALM	wk-str	1.4

TABLE 3. (CONTINUED)

DATE	UTC	STATION	CHARACTER	SNR
960125	2043	RAYN	strong	2.4
960126	1311	HALM	strong	1.5
960126	1311	RAYN	strong	1.5
960126	1702	HALM	strong	1.5
960126	1702	RAYN	strong	1.7
960126	1901	HALM	weak	
960126	1901	RAYN	weak	1.0
960128	0843	HALM	strong	1.6
960128	0843	RANI	weak	1.2
960128	0843	RAYN	strong	1.7
960131	2043	HALM	weak	1.0
960131	2043	RAYN	weak	1.1
960205	0828	RANI	blocked	
960216	0250	HALM	blocked	
960216	0250	RAYN	weak	
960216	2140	HALM	blocked	
960216	2140	RAYN	weak	1.1
960225	1614	HALM	blocked	
960225	1742	HALM	blocked	
960225	1742	RANI	blocked	
960225	1742	SODA	blocked	
960303	0845	RAYN	weak	1.6
960304	0135	RAYN	blocked	
960304	0135	SODA	weak	0.9
960307	0328	RAYN	weak	1.0
960308	0148	AFIF	strong	2.9
960308	0148	HALM	strong	3.0
960308	0148	RAYN	strong	4.6
960313	0805	AFIF	strong	2.1
960313	0805	HALM	weak	0.9
960313	0805	RAYN	strong	1.6
960316	0231	HALM	blocked	
960316	0231	RAYN	blocked	
960316	0324	RAYN	weak	1.4
960316	2018	AFIF	weak	1.1
960316	2018	HALM	strong	1.7
960316	2018	RAYN	strong	1.2
960318	0311	AFIF	weak	0.9
960318	0311	HALM	strong	2.1
960318	0311	RANI	weak	1.1
960318	0311	RAYN	strong	1.3
960320	0154	HALM	weak	1.6
960320	0154	RAYN	strong	1.8
960320	2224	AFIF	weak	1.1
960320	2224	HALM	strong	1.9
960320	2224	RANI	weak	1.5
960320	2224	RAYN	strong	1.9
960320	2224	SODA	blocked	
960323	0402	AFIF	weak	1.0
960323	0402	HALM	weak	1.3
960323	0402	RAYN	strong	2.2

TABLE 3. (CONTINUED)

DATE	UTC	STATION	CHARACTER	SNR
960327	0333	AFIF	strong	1.6
960327	0333	HALM	strong	1.7
960327	0333	RANI	strong	1.5
960327	0333	RAYN	strong	2.7
960331	1507	HALM	weak	1.2
960331	1507	RAYN	strong	1.4
960331	1602	AFIF	weak	1.1
960331	1602	HALM	weak	1.1
960331	1602	RAYN	wk-str	1.7
960331	2113	AFIF	weak	1.5
960331	2113	HALM	wk-str	1.7
960331	2113	RANI	strong	1.3
960331	2113	RAYN	wk-str	1.2
960402	1041	AFIF	weak	0.7
960402	1041	HALM	weak	1.2
960402	1041	RAYN	wk-str	1.4
960409	1738	HALM	weak	1.3
960409	1738	RAYN	weak	1.1
960410	2026	AFIF	weak	1.1
960410	2026	HALM	weak	1.3
960410	2026	RAYN	strong	1.6
960410	2150	RAYN	weak	1.1
960411	2000	AFIF	weak	0.9
960411	2000	HALM	weak	1.1
960411	2000	RAYN	weak	1.3
960415	1410	HALM	weak	1.0
960415	1410	RAYN	strong	1.5
960418	2013	HALM	weak	1.2
960418	2013	RAYN	blocked	
960420	1830	AFIF	strong	2.9
960420	1830	HALM	strong	3.3
960420	1830	RAYN	strong	5.2
960501	2242	HALM	weak	
960501	2242	RAYN	wk-str	0.8
960503	0736	AFIF	blocked	
960503	0736	HALM	blocked	
960503	0736	RAYN	blocked	
960506	1018	HALM	strong	1.8
960506	1018	RAYN	strong	2.4
960510	1523	AFIF	weak	1.3
960510	1523	HALM	weak	1.0
960510	1523	RAYN	weak	1.2
960518	2010	AFIF	blocked	
960518	2010	HALM	blocked	
960524	0635	AFIF	weak	1.3
960524	0635	HALM	strong	1.9
960524	0635	RANI	weak	1.3
960525	1700	AFIF	weak	1.2
960525	1700	HALM	blocked	
960525	1700	RANI	blocked	
960529	0924	HALM	strong	2.2

TABLE 3. (CONTINUED)

DATE	UTC	STATION	CHARACTER	SNR
960602	1242	AFIF	weak	1.4
960602	1242	HALM	weak	1.2
960607	0503	AFIF	blocked	
960607	0503	HALM	blocked	
960607	0517	AFIF	weak	0.9
960618	1917	HALM	weak	
960618	1917	RIYD	weak	1.4
960618	1917	UQSK	weak	1.2
960701	0814	AFIF	weak	1.1
960701	0814	HALM	strong	1.6
960701	0814	RIYD	strong	2.1
960701	0814	UQSK	strong	1.8
960715	1931	AFIF	blocked	
960715	1931	HALM	weak	1.2
960715	1931	RIYD	weak	1.2
960715	1931	UQSK	weak	
960716	0840	AFIF	wk-str	1.1
960716	0840	HALM	weak	1.4
960716	0840	RIYD	strong	1.3
960716	0840	UQSK	strong	2.0
960716	1646	AFIF	weak	1.4
960716	1646	HALM	weak	1.5
960716	1646	RIYD	strong	1.2
960716	1646	UQSK	strong	2.2
960721	1118	AFIF	weak	1.3
960721	1118	HALM	weak	1.0
960721	1118	RIYD	strong	2.3
960721	1118	UQSK	weak	
960806	2027	AFIF	weak	1.2
960806	2027	HALM	weak	0.7
960806	2027	RIYD	strong	3.3
960806	2027	SODA	blocked	
960806	2027	TAIF	weak	1.3
960806	2027	UQSK	weak	1.4
960812	2358	AFIF	weak	1.6
960812	2358	HALM	strong	1.7
960812	2358	UQSK	strong	1.2
960824	0515	AFIF	weak	1.5
960824	0515	HALM	blocked	
960824	0515	RIYD	weak	
960824	0515	UQSK	weak	
960825	0053	AFIF	weak	1.2
960825	0053	HALM	weak	1.6
960825	0053	RIYD	strong	2.0
960825	0053	UQSK	strong	1.6
960904	2039	AFIF	weak	
960904	2039	HALM	weak	1.1
960906	1236	AFIF	strong	1.6
960906	1236	HALM	strong	2.5
960906	1236	RIYD	strong	2.5
960906	1236	UQSK	strong	1.4

TABLE 3. (CONTINUED)

DATE	UTC	STATION	CHARACTER	SNR
960914	1909	HALM	weak	
960914	1909	RIYD	strong	1.4
960914	1909	UQSK	weak	1.6
960916	0113	HALM	weak	
960920	2158	AFIF	weak	
960925	1622	AFIF	weak	2.2
960925	1622	HALM	strong	2.6
960925	1622	RIYD	strong	5.5
960925	1622	SODA	weak	1.2
960925	1622	UQSK	strong	2.4
960926	0955	AFIF	weak	1.2
960926	0955	HALM	weak	1.0
960926	0955	RIYD	weak	1.2
960926	0955	SODA	weak	1.3
960926	0955	UQSK	weak	1.5
960928	1353	HALM	blocked	
960928	1353	UQSK	blocked	
960929	2119	HALM	weak	1.2
960929	2119	RIYD	weak	1.2
960929	2119	UQSK	weak	1.9
961004	1607	HALM	weak	
961004	1607	UQSK	weak	1.0
961015	2110	RIYD	blocked	
961015	2110	UQSK	weak	0.9
961018	0926	HALM	blocked	
961018	0926	RIYD	blocked	
961018	0926	SODA	weak	
961018	0926	UQSK	blocked	
961027	0141	HALM	blocked	
961027	0141	RIYD	weak	1.5
961027	0141	UQSK	strong	2.8
961108	0505	HALM	strong	1.1
961108	0505	UQSK	strong	1.9
961118	1152	HALM	strong	1.9
961118	1152	RIYD	strong	1.8
961118	1152	SODA	blocked	
961118	1152	UQSK	strong	3.2
961124	1235	HALM	strong	
961124	1235	RIYD	strong	1.7
961124	1235	UQSK	strong	2.1
961124	1834	HALM	strong	2.3
961124	1834	RIYD	strong	3.7
961124	1834	UQSK	strong	1.1
961204	0239	HALM	strong	1.8
961204	0239	RIYD	strong	11.8
961204	0239	SODA	weak	1.6
961204	0239	UQSK	strong	4.3
961209	0233	UQSK	weak	1.4
961214	1949	AFIF	weak	1.7
961214	1949	RIYD	strong	4.0
961214	1949	SODA	blocked	

TABLE 3. (CONTINUED)

DATE	UTC	STATION	CHARACTER	SNR
961214	1949	UQSK	strong	2.6
961219	2320	RIYD	weak	1.7
961219	2320	UQSK	weak	1.1
961220	0018	AFIF	weak	1.9
961220	0018	RIYD	strong	2.8
961220	0018	SODA	blocked	
961220	0018	UQSK	strong	2.6
961220	0612	RIYD	strong	2.7
961220	0612	UQSK	strong	1.7
961220	0808	UQSK	wk-str	1.6
961221	0332	AFIF	strong	2.4
961221	0332	RIYD	strong	1.9
961221	0332	UQSK	strong	1.2
961221	2313	AFIF	weak	
961221	2313	RIYD	blocked	
961221	2313	UQSK	weak	
961226	0917	AFIF	blocked	
961226	0917	RIYD	weak	
961226	0917	UQSK	weak	1.3
961231	2317	UQSK	weak	
970113	0224	HALM	weak	
970115	1528	AFIF	weak	0.8
970115	1528	HALM	weak	1.2
970115	1528	RIYD	weak	1.0
970115	1528	UQSK	weak	0.8
970118	1320	AFIF	weak	1.5
970118	1320	HALM	strong	1.8
970118	1320	RIYD	weak	
970118	1320	UQSK	strong	2.6
970119	1906	UQSK	strong	1.9
970124	1712	AFIF	blocked	
970124	1712	UQSK	blocked	
970204	0953	AFIF	blocked	
970204	0953	HALM	blocked	
970204	0953	RANI	blocked	
970204	0953	RIYD	blocked	
970204	0953	SODA	blocked	
970204	0953	UQSK	blocked	
970204	1037	AFIF	blocked	
970204	1037	HALM	blocked	
970204	1037	RANI	blocked	
970204	1037	RIYD	blocked	
970204	1037	SODA	blocked	
970204	1037	UQSK	blocked	
970205	0753	AFIF	blocked	
970205	0753	HALM	blocked	
970205	0753	RANI	blocked	
970205	0753	SODA	blocked	
970205	0753	UQSK	blocked	
970208	0328	AFIF	blocked	
970208	0328	HALM	weak	

TABLE 3. (CONTINUED)

DATE	UTC	STATION	CHARACTER	SNR
970208	0328	RIYD	weak	1.2
970208	0328	UQSK	weak	
970210	0427	AFIF	weak	
970210	0427	HALM	weak	
970210	0427	RIYD	strong	1.6
970210	0427	UQSK	weak	1.2
970211	1842	AFIF	blocked	
970211	1842	HALM	blocked	
970211	1842	RIYD	weak	1.2
970211	1842	UQSK	blocked	
970212	1442	HALM	weak	
970212	1442	RIYD	weak	1.0
970212	1442	UQSK	weak	1.1
970212	1700	HALM	weak	1.0
970212	1700	RIYD	strong	1.2
970215	1947	AFIF	weak	
970215	1947	HALM	weak	2.1
970215	1947	RANI	blocked	
970215	1947	RIYD	strong	2.5
970215	1947	SODA	blocked	
970215	1947	UQSK	strong	1.6
970217	0431	AFIF	blocked	
970217	0431	HALM	blocked	
970217	0431	RANI	weak	1.3
970217	0431	RIYD	blocked	
970217	0431	SODA	blocked	
970217	0431	UQSK	weak	1.0
970217	0450	AFIF	weak	2.0
970217	0450	HALM	weak	1.6
970217	0450	RIYD	weak	1.2
970217	0450	UQSK	weak	0.9

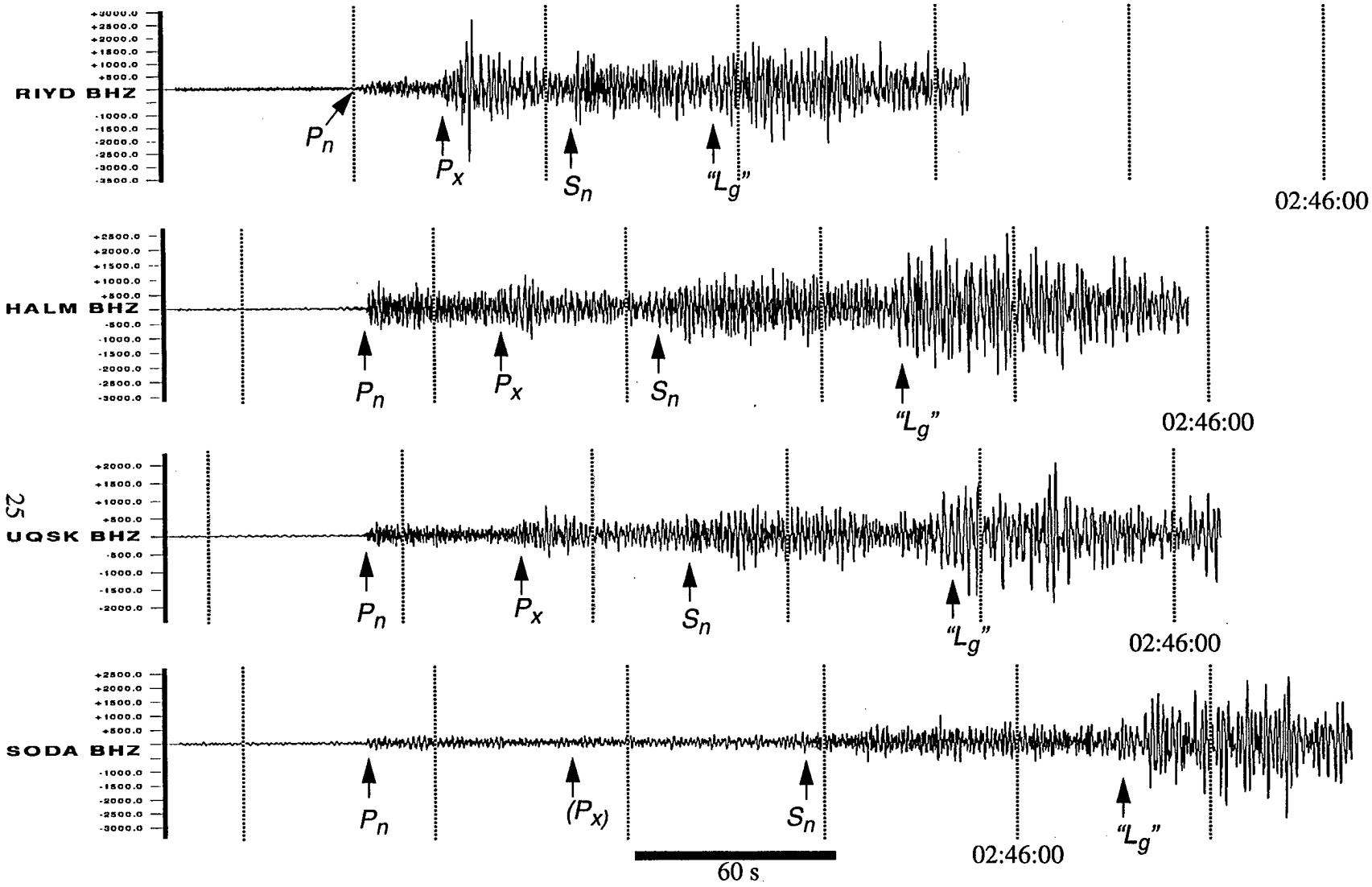

Figure 8. (a) Broadband vertical seismograms for a single event showing very strong P_x. Seismograms have been bandpass filtered between 0.5 and 10 Hz. The RIYD seismogram has the strongest P_x observed in our study (SNR 11.8). Note the rapidly decreasing strength of P_x with distance, and the strong "L_g" phase (which actually has a velocity of about 3.2 km/sec).

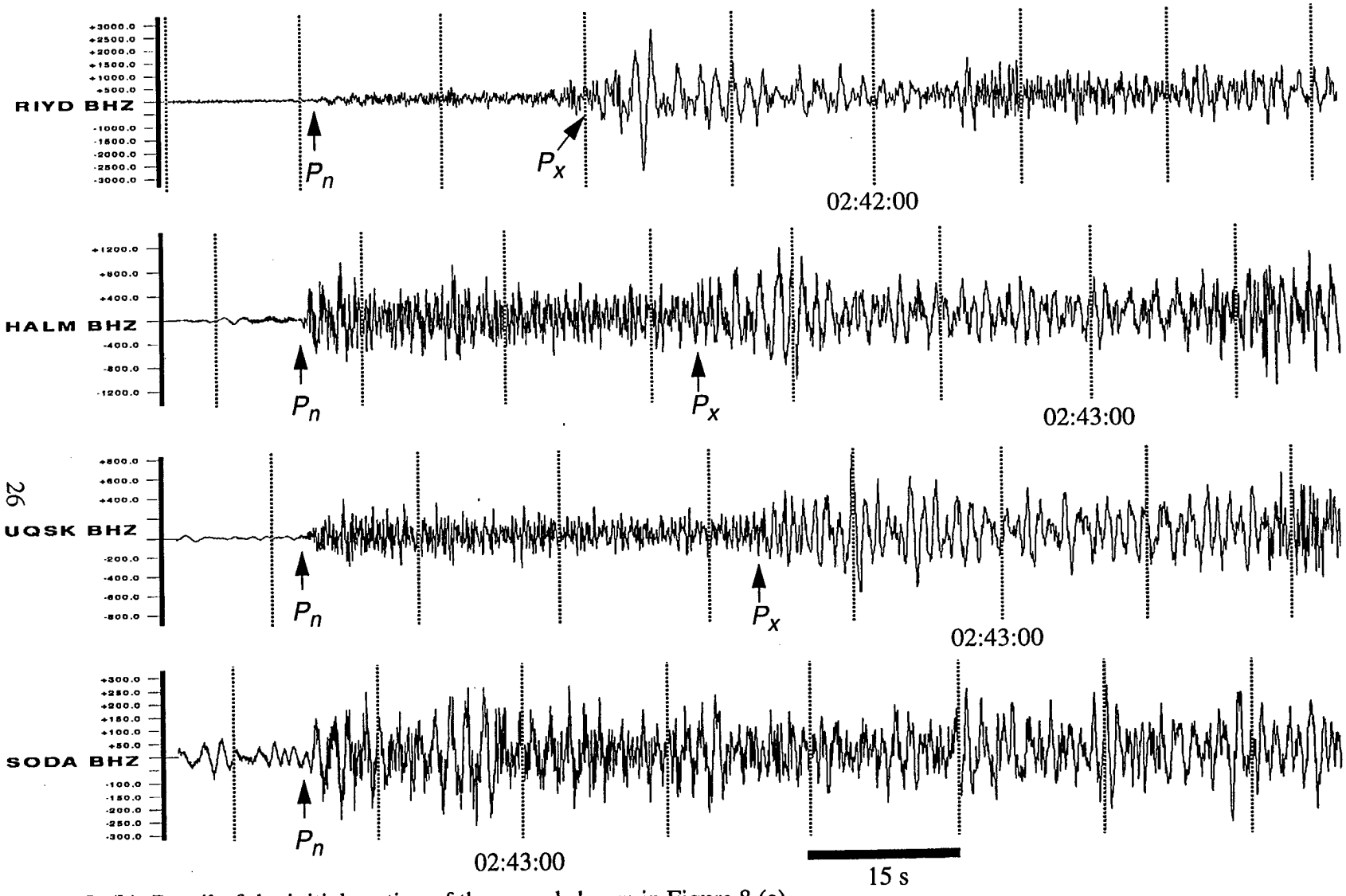

Figure 8. (b) Detail of the initial portion of the record shown in Figure 8 (a).

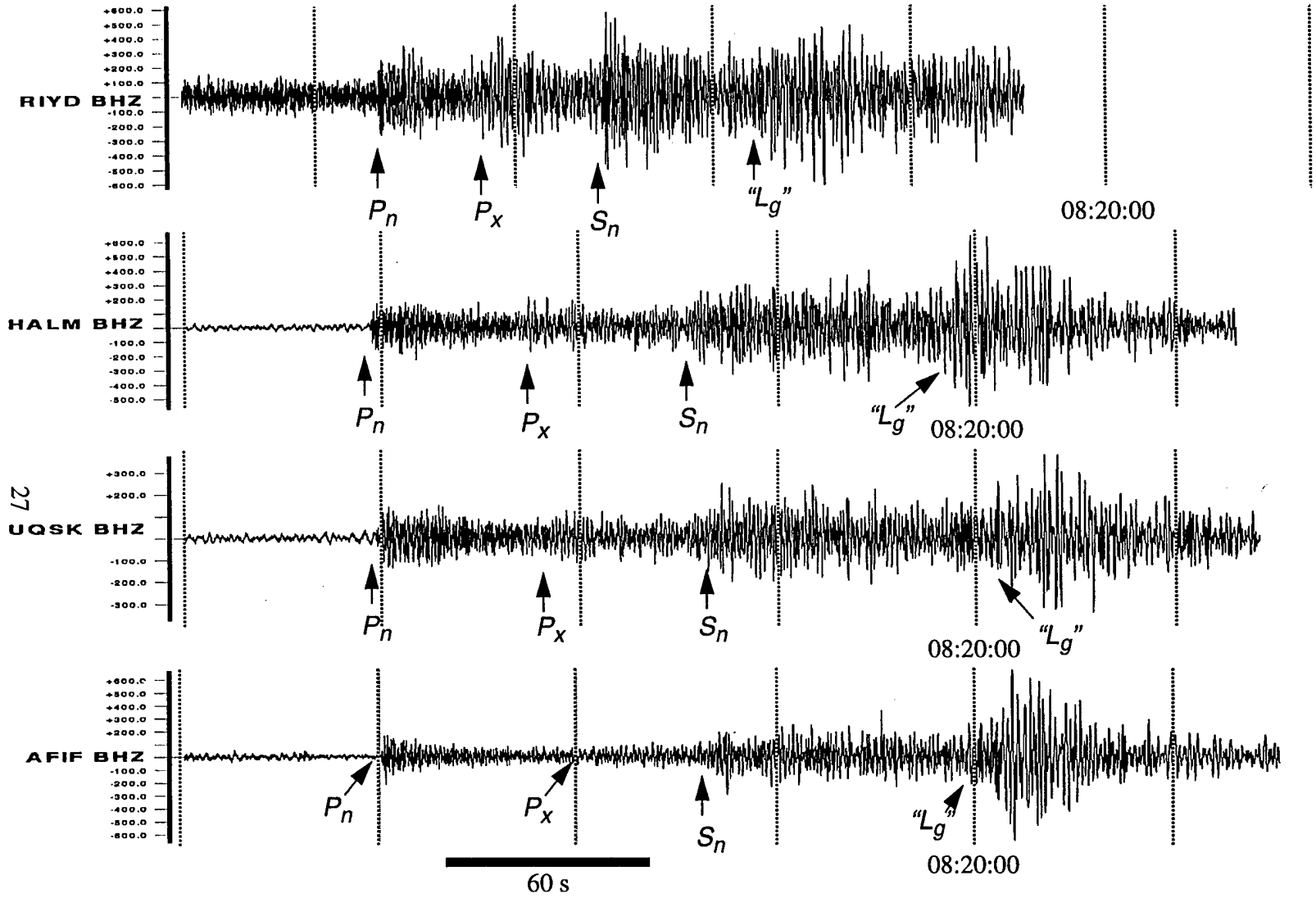

Figure 9. (a) Broadband vertical seismograms for a single event showing a fairly typical P_x. Seismograms have been filtered with a high pass corner at 0.5 Hz. Note the strong "L_g" arrivals.

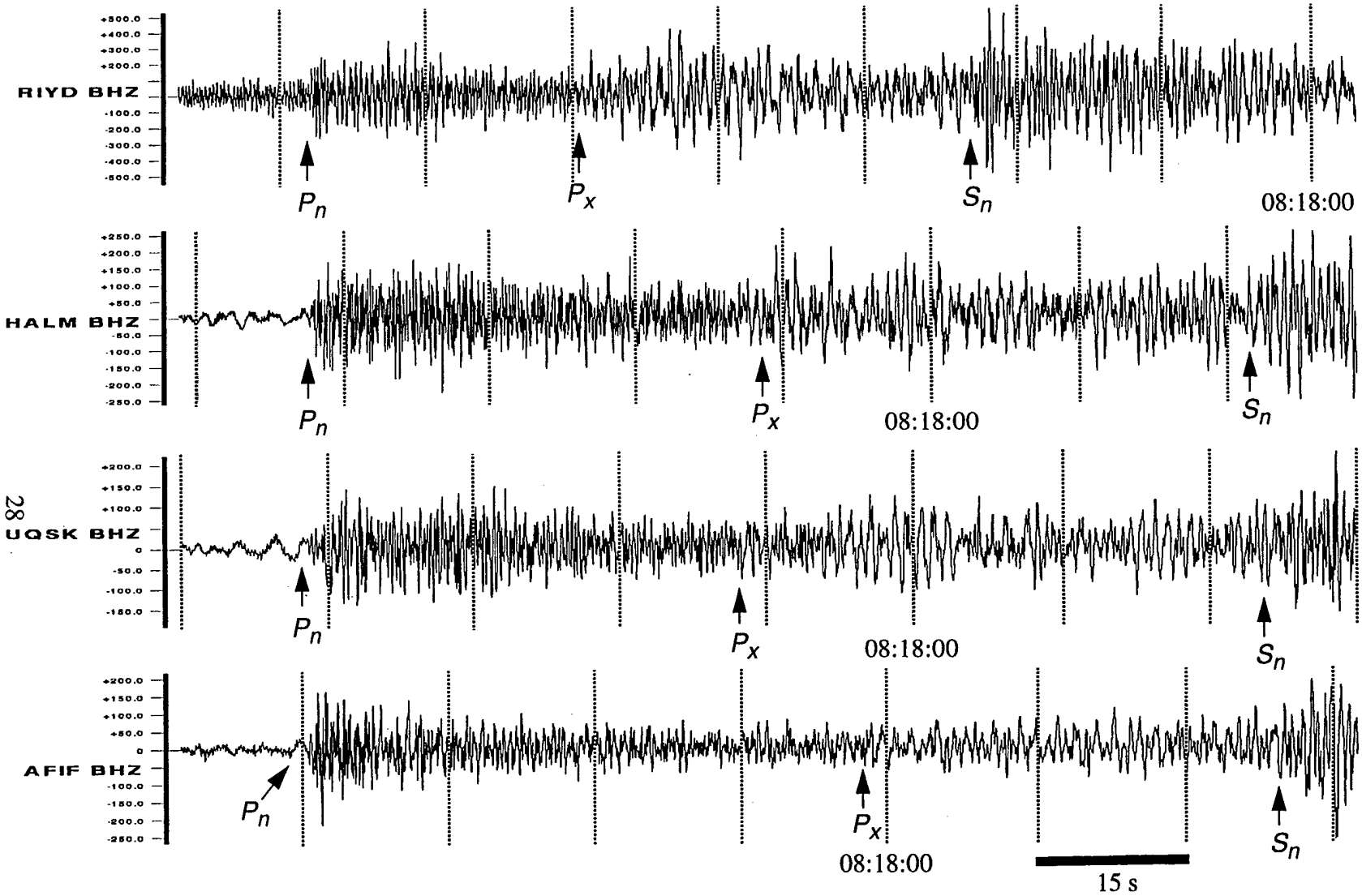

Figure 9. (b) Detail of the initial portion of the record shown in Figure 9 (a).

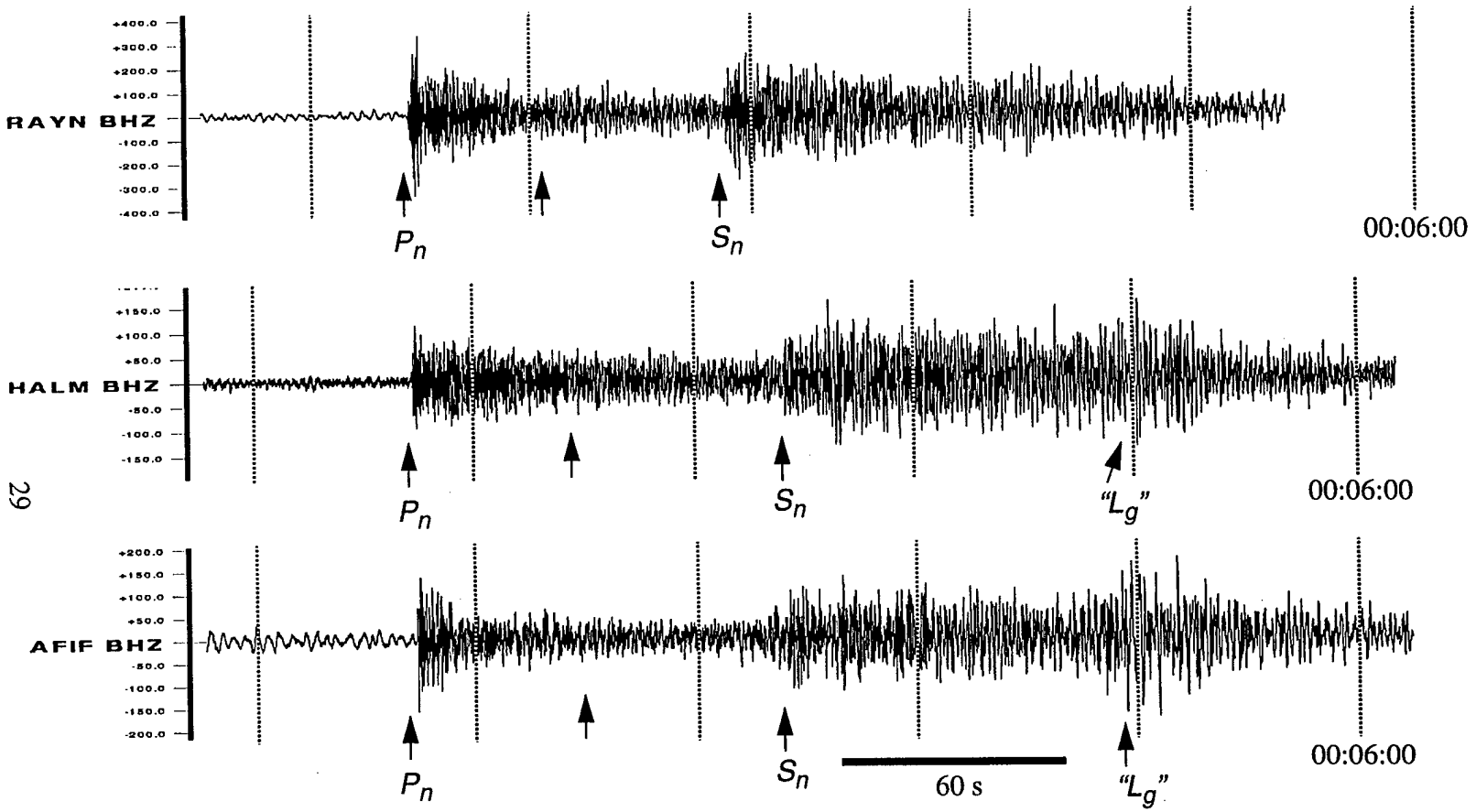

Figure 10. (a) Broadband vertical seismograms for a single event showing an absence or near-absence of observable P_x at all stations. Seismograms have been bandpass filtered between 0.5 and 10 Hz. Note that while P_x (expected near unlabeled arrows) appears to be absent, two stations appear to show an "L_g" arrival.

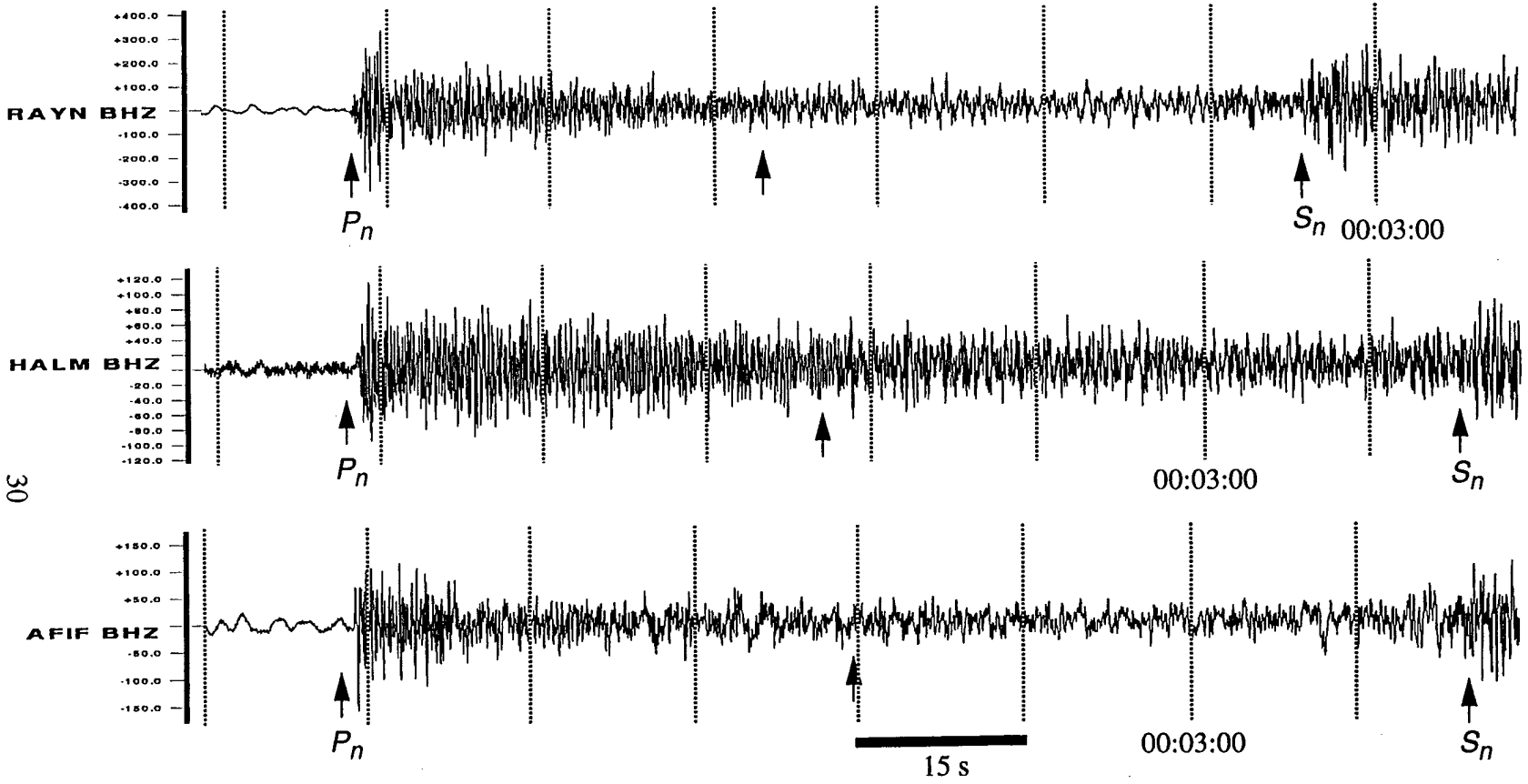

Figure10 (b). Detail of the initial portion of the record shown in Figure 10 (a).

trace of P_x. These seismograms were classified as "blocked", with the understanding that there is certainly some unavoidable overlap between this category and the lower SNR limits of the "weak" category.

With this classification scheme it is possible to look at the geographic distribution of paths displaying the different P_x wave phenomena. Figure 11 shows that the very strong observations are confined to relatively short paths that have either no Arabian Shield component or only a very short one. Four of the seven observations of a very strong P_x come from RIYD (Riyadh), which is not located on the Arabian Shield but on the Arabian Platform.

Strong observations of P_x are mainly confined to paths from the Zagros to eastern Arabian Shield stations. There is a long range observation for a path to the north, as well as one that nearly crosses the shield. It is notable, however, that the P_x phase typically is not strongly observed by the stations in the western shield.

Weak P_x is observed at all stations. A careful comparison of the path diagrams for the strong and weak cases shows that the weak and strong observations have paths that overlap each other and sources that substantially overlap, but the sources for observed weak P_x often occur slightly farther east in the Zagros than the sources for strong P_x. This hints that there is a blockage effect going on, with P_x severely attenuated or absent for sources beyond somewhere in the central Zagros. This observation is borne out by the location of paths for which P_x is blocked, which almost invariably are longer than the paths for the weak or the strong observations. Many of the blocked paths cross the entire Zagros Fold Belt.

Cases in which P_x is apparently blocked at a station are uncommon, accounting for only about 25% of our observations. Cases in which P_x is apparently blocked at all stations are rare. For only 13 events for which there were two or more observing stations did we find P_x was blocked at all stations that observed that event (with the additional condition that if only two stations observed an event, both stations had to be among the 5 easternmost stations RIYD, RAYN,

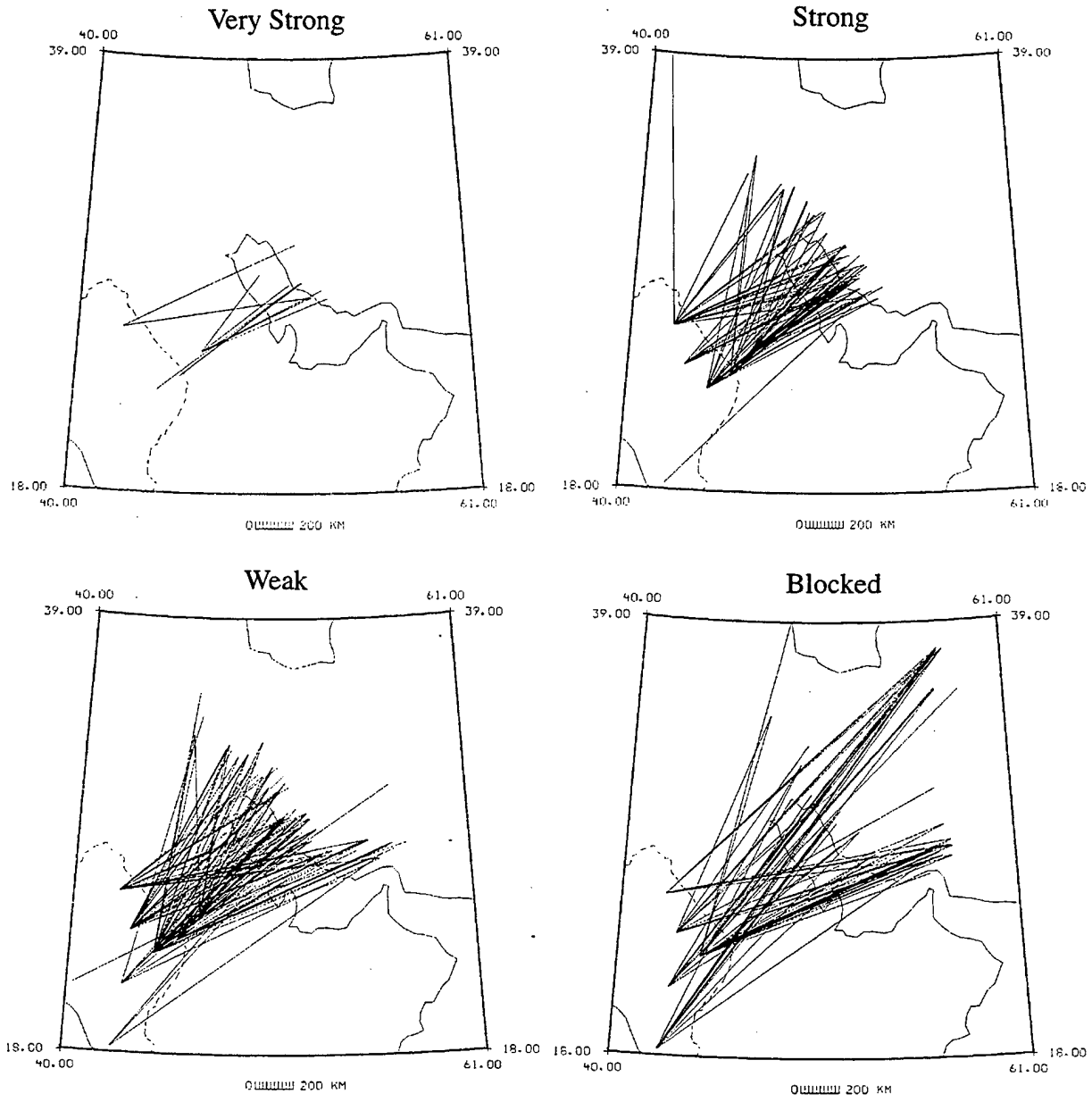

Figure 11. Event-station paths for the seismograms analyzed in this study. The paths are plotted according to differing observed strengths of the P_x phase as follows: very strong, P_x SNR greater than 3; strong, P_x SNR between 1.6 and 3; weak, P_x observable but SNR 1.5 or less; and blocked, P_x apparently absent on all components.

HALM, AFIF, and UQSK). These events are plotted in Figure 12 and listed in Table 4. All but two of the events for which P_x blockage is observed at all recording stations occur east of the Zagros Fold Belt, indicating that the blockage in these cases is likely to be due to wave guide disruption in the Zagros.

There are several additional events for which P_x blockage is observed at one or more stations, but not all. We believe that these events and the two in the western Zagros for which all stations observed blocked P_x may be deeper events than normal for the area. PDE focal depths for the events occurring during the Saudi deployment were generally free solutions without the constraint of depth phases. Figure 13 shows PDE events (1973 - 1997) whose depths were computed from pP - P intervals and are thus likely to be more reliable than free depth solutions. This figure shows that there are relatively few events with reliably calculated lower crustal or subcrustal depths (say 35 km or more), and confirms that it is possible that some cases of P_x blockage may be due to deeper than normal focal depth. Depending on the mechanism by which P_x is generated, it is possible that events for which P_x is weak may also be comparatively deep. For example, it may be possible for a weak P_x to be generated by an event below the waveguide if the P wave incident to the waveguide is reflected at the top of the waveguide, leading to multiple internal reflections. Generation of such a wave is highly dependent upon the details of crustal structure, and our present knowledge of these details is probably inadequate to judge whether or not such a phase exists.

Using PDE hypocentral determinations, an average velocity for the P_x phase was obtained assuming that the intercept time is zero. The velocity determinations are affected by errors in the hypocenters and origin times as well as picking errors. Epicentral errors of the order of 25 km and combined origin time/picking errors of 10 s are likely to contaminate the data set. Nevertheless, the long ray paths lead to relatively small average velocity determination errors, on the order of 5-10% or less. Figure 14 shows that the P_x phase has an apparent velocity of about 5.7 km/sec. This is considerably slower than expected for P_g, but is a velocity that would be reasonable for a guided P wave in the upper crustal sedimentary formations of the Arabian

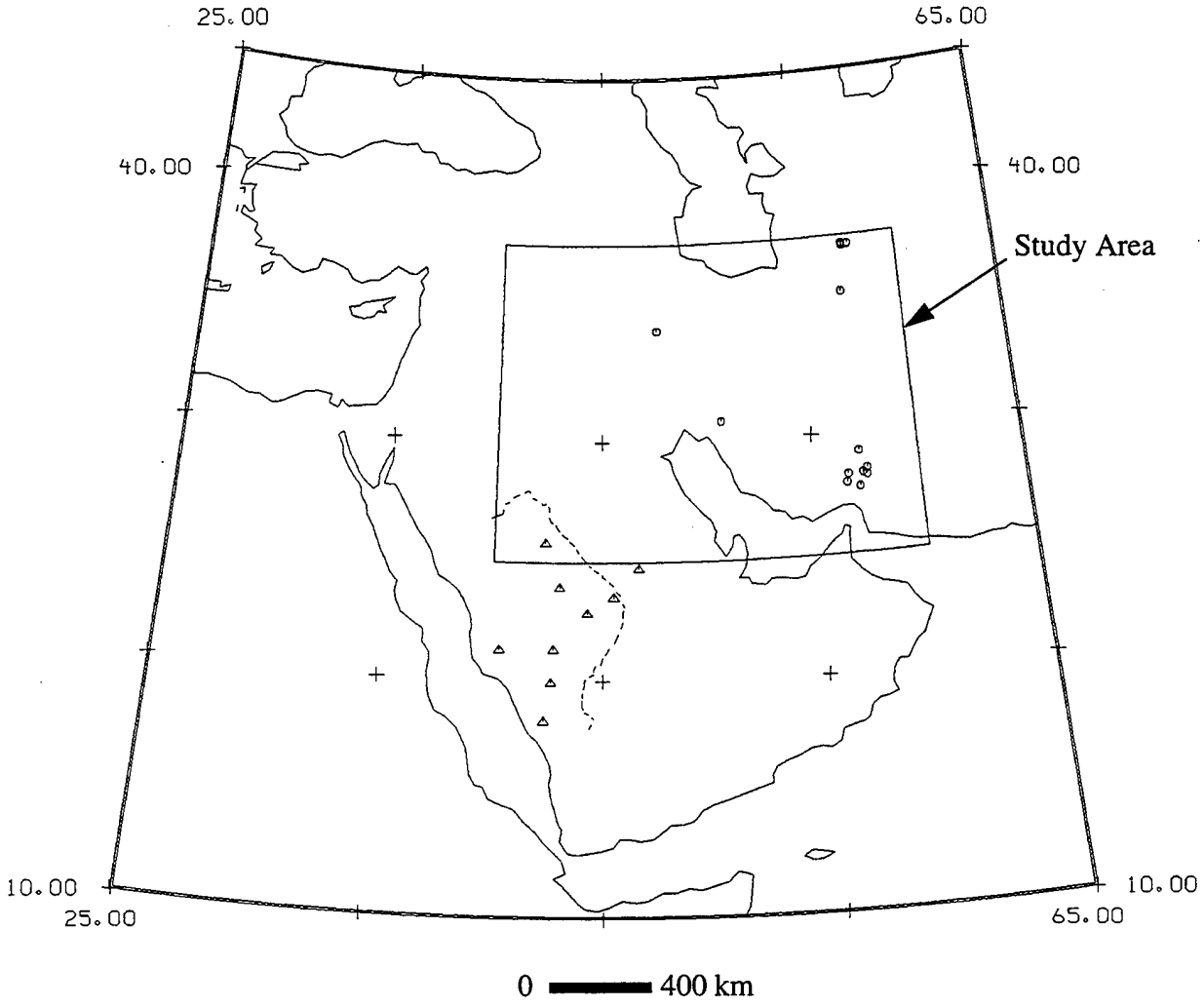

Figure 12. Locations of events apparently having blocked P_x at all stations.

TABLE 4
PDE LOCATIONS FOR EVENTS WITH "BLOCKED" Px

YEAR	MO	DA	TIME	N LAT	E LONG	DEPTH		MB
1995	12	21	073900.25*	27.751	57.145	33	N	4.1
1995	12	28	182335.09	27.948	56.552	46	*	4.6
1996	01	13	095717.64	28.326	57.325	33	N	4.3
1996	02	25	174204.66	35.685	57.038	33	N	4.9
1996	03	16	023143.52*	28.291	56.631	33	N	4.0
1996	05	03	073642.50*	29.210	57.208	33	N	4.2
1996	05	18	201022.74*	34.479	47.684	33	N	3.8
1996	06	07	050320.70	30.759	50.717	33	N	4.7
1996	09	28	135355.89	28.481	57.555	33	N	4.8
1997	01	24	171257.58	28.226	57.529	39	D	4.5
1997	02	04	095355.73	37.564	57.295	10	G	5.3
1997	02	04	103747.14	37.661	57.291	10	G	5.9
1997	02	05	075345.62	37.629	57.594	10	G	5.2

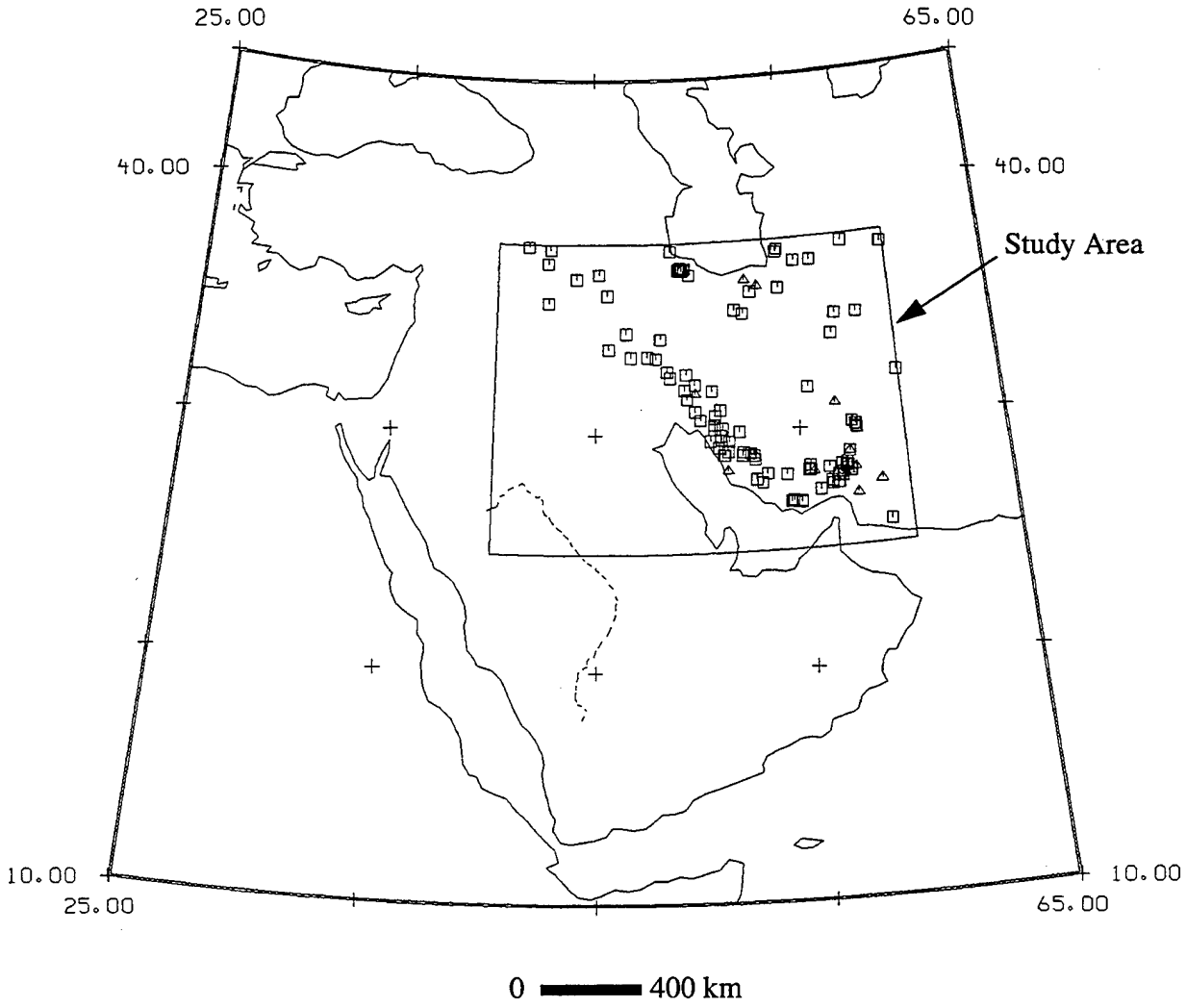

Figure 13. PDE locations of Zagros region events, 1973 - 1997 having depths constrained by *pP* - *P* intervals. Depths from 0 - 35 km are denoted by square symbols while events at greater depths are shown by triangles.

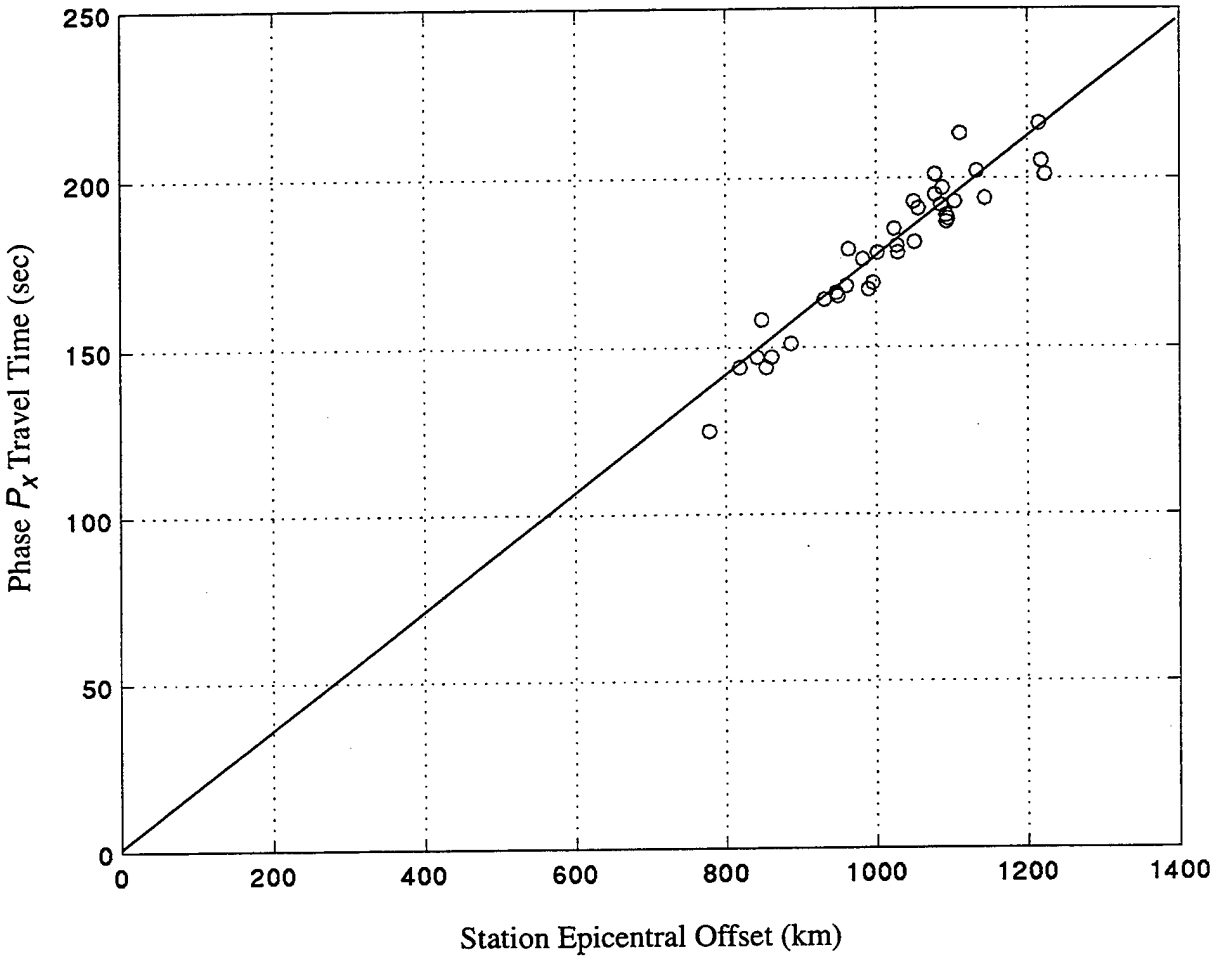

Figure 14. Observed (distance, time) pairs for P_x. Distance and time are calculated from PDE location and origin time. Estimated uncertainties are 25 km in epicentral distance and 10 sec in time. The plotted line represents a velocity of 5.7 km/s.

Platform.

Some hypothetical ray paths for the P_x phase are sketched in Figure 15. We believe that strong P_x phases may benefit from source-receiver paths that lie entirely within one layer of the upper Arabian Platform.

Discussion

The observed P_x phase has two characteristics that indicate it is a guided wave in the upper crust. First, its apparent velocity of around 5.7 km/sec is lower than the usual P_g velocity and is also too low to conceivably be due to any reflected phase, given the long distances at which it is observed. Second, its low frequency content indicates attenuation that can only occur through paths at shallow depths, given the high frequencies observed for P_n at long distances.

While we did not make a study of the L_g phase, we note that it appears that L_g propagates slowly in the same region that we observe P_x. While it would be tempting to say that they are analogous guided waves, Figure 10a shows apparent L_g arrivals at two stations where P_x appears to be blocked and for which there is no other crustal P wave recorded which could correspond to the apparent L_g arrival.

We suspect there are at least four mechanisms involved in controlling the relative strength of the P_x phase:

(1) blockage by the Zagros Fold Belt for most sources to the east of the Zagros;

(2) hypocenter focal depth, with subcrustal events generating P_x weakly or not at all;

(3) distance travelled in the Arabian Shield, with P_x apparently propagating poorly for shield paths exceeding about 100 km;

(4) focal mechanism.

Our study gives at least circumstantial evidence for the influence of the first three mechanisms.

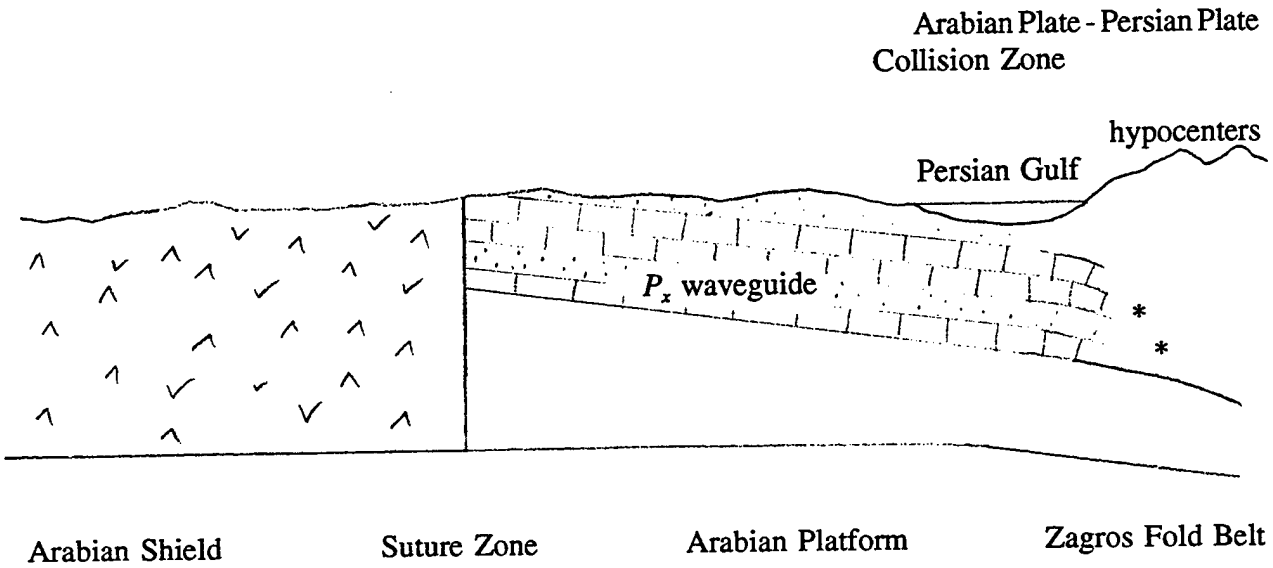

Figure 15. Cartoon of our interpretation of the P_x waveguide (not to scale).

We could not investigate focal mechanism as a possible factor due to the small number and wide distribution of mechanisms available for Zagros region events occurring during the Saudi deployment, but it seems likely that it plays a role in P_x amplitudes.

Our choice of terminology in calling the P_x phase something other than P_g may be questioned, but is based on the practical difficulty that were it to be called P_g, the same phase designation would refer to phases with different velocities, travelling in different layers in different parts of the Arabian Plate. Furthermore, the rapid decrease in amplitude of P_x with distance travelled in the Arabian Shield suggests that the wave guide is not continuous and that there is an impedance barrier to the transmission of energy from the P_x wave guide into the rocks of the upper Arabian Shield.

The P_x phase, since it appears to be a guided wave in the upper crust, has potential for use in focal depth determination and therefore has implications for monitoring the Comprehensive Test Ban Treaty. If P_x is generated in a manner analogous to P_g, then it has a near-horizontal angle of incidence at long distances and therefore its travel time will be essentially independent of focal depth. P_n, on the other hand, has a travel time dependent on focal depth because of its angle of incidence and its intercept time being a function of depth. Therefore, P_n - P_x intervals are likely to be functions of focal depth. P_n - P_x as observed in the Arabian Peninsula should be a more sensitive function of depth than P_g - P_n elsewhere, because P_x's relatively slow velocity will lead to longer P_x - P_n lapse times at equivalent distances than could be expected for P_g - P_n. However, it should be noted that our data set suggests that the Arabian Shield may not be the place to most efficiently monitor P_x. Observations at RIYD, on the Arabian Platform, indicate that good sites on the Arabian Platform could out-perform shield sites; they also have the advantage of shorter event-station paths and may therefore be capable of lower magnitude detection thresholds.

References

Jackson, J., and T. Fitch (1981), Basement faulting and the focal depths of the larger earthquakes in the Zagros mountains (Iran), *Geophysical Journal of the Royal Astronomical Society* **64**, 561-

586.

Mooney, W. D., M. E. Gettings, H. R. Blank, and J. H. Healy (1985), Saudi Arabian seismic-refraction profile: A traveltime interpretation of crustal and upper mantle structure, *Tectonophysics* **111**, 173-246.

Vernon, F. L., R. J. Mellors, J. Berger, A. M. Al-Amri, and J. Zollweg (1996), Initial results from the deployment of broadband seismometers in the Saudi Arabian Shield, *in* Lewkowicz, J. F., J. M. McPhetres, and D. T. Reiter (eds.), *Proceedings of the 18th Annual Seismic Research Symposium on Monitoring a Comprehensive Test Ban Treaty, 4-6 September 1996*, Phillips Laboratory Report PL-TR-96-2153, 809-818, ADA 313692.

THOMAS AHRENS
SEISMOLOGICAL LABORATORY 252-21
CALIFORNIA INST. OF TECHNOLOGY
PASADENA, CA 91125

AIR FORCE RESEARCH LABORATORY
ATTN: VSOP
29 RANDOLPH ROAD
HANSCOM AFB, MA 01731-3010 (2 COPIES)

AIR FORCE RESEARCH LABORATORY
ATTN: RESEARCH LIBRARY/TL
5 WRIGHT STREET
HANSCOM AFB, MA 01731-3004

AIR FORCE RESEARCH LABORATORY
ATTN: AFRL/SUL
3550 ABERDEEN AVE SE
KIRTLAND AFB, NM 87117-5776 (2 COPIES)

RALPH ALEWINE
NTPO
1901 N. MOORE STREET, SUITE 609
ARLINGTON, VA 22209

G. ELI BAKER
MAXWELL TECHNOLOGIES
8888 BALBOA AVE.
SAN DIEGO, CA 92123-1506

MUAWIA BARAZANGI
INSTOC
3126 SNEE HALL
CORNELL UNIVERSITY
ITHACA, NY 14853

DOUGLAS BAUMGARDT
ENSCO INC.
5400 PORT ROYAL ROAD
SPRINGFIELD, VA 22151

THERON J. BENNETT
MAXWELL TECHNOLOGIES
11800 SUNRISE VALLEY
SUITE 1212
RESTON, VA 22091

WILLIAM BENSON
NAS/COS
ROOM HA372
2001 WISCONSIN AVE. NW
WASHINGTON DC 20007

JONATHAN BERGER
UNIV. OF CALIFORNIA, SAN DIEGO
SCRIPPS INST. OF OCEANOGRAPHY IGPP, 0225
9500 GILMAN DRIVE
LA JOLLA, CA 92093-0225

ROBERT BLANDFORD
AFTAC
1300 N. 17TH STREET
SUITE 1450
ARLINGTON, VA 22209-2308

LESLIE A. CASEY
DEPT. OF ENERGY/NN-20
1000 INDEPENDENCE AVE. SW
WASHINGTON DC 20585-0420

CENTER FOR MONITORING RESEARCH
ATTN: LIBRARIAN
1300 N. 17th STREET, SUITE 1450
ARLINGTON, VA 22209

FRANCESCA CHAVEZ
LOS ALAMOS NATIONAL LAB
P.O. BOX 1663, MS-D460
LOS ALAMOS, NM 87545 (5 COPIES)

ANTON DAINTY
DTRA/PMA
45045 AVIATION DRIVE
DULLESVA 20166-7517

CATHERINE DE GROOT-HEDLIN
UNIV. OF CALIFORNIA, SAN DIEGO
IGPP
8604 LA JOLLA SHORES DRIVE
SAN DIEGO, CA 92093

DIANE DOSER
DEPT. OF GEOLOGICAL SCIENCES
THE UNIVERSITY OF TEXAS AT EL PASO
EL PASO, TX 79968

DTIC
8725 JOHN J. KINGMAN ROAD
FT BELVOIR, VA 22060-6218 (2 COPIES)

MARK D. FISK
MISSION RESEARCH CORPORATION
735 STATE STREET
P.O. DRAWER 719
SANTA BARBARA, CA 93102-0719

LORI GRANT
MULTIMAX, INC.
311C FOREST AVE. SUITE 3
PACIFIC GROVE, CA 93950

HENRY GRAY
SMU STATISTICS DEPARTMENT
P.O. BOX 750302
DALLAS, TX 75275-0302

I. N. GUPTA
MULTIMAX, INC.
1441 MCCORMICK DRIVE
LARGO, MD 20774

DAVID HARKRIDER
BOSTON COLLEGE
24 MARTHA'S PT. RD.
CONCORD, MA 01742

THOMAS HEARN
NEW MEXICO STATE UNIVERSITY
DEPARTMENT OF PHYSICS
LAS CRUCES, NM 88003

MICHAEL HEDLIN
UNIVERSITY OF CALIFORNIA, SAN DIEGO
SCRIPPS INST. OF OCEANOGRAPHY
9500 GILMAN DRIVE
LA JOLLA, CA 92093-0225

DONALD HELMBERGER
CALIFORNIA INST. OF TECHNOLOGY
DIV. OF GEOL. & PLANETARY SCIENCES
SEISMOLOGICAL LABORATORY
PASADENA, CA 91125

EUGENE HERRIN
SOUTHERN METHODIST UNIVERSITY
DEPT. OF GEOLOGICAL SCIENCES
DALLAS, TX 75275-0395

ROBERT HERRMANN
ST. LOUIS UNIVERSITY
DEPT. OF EARTH & ATMOS. SCIENCES
3507 LACLEDE AVENUE
ST. LOUIS, MO 63103

VINDELL HSU
HQ/AFTAC/TTR
1030 S. HIGHWAY A1A
PATRICK AFB, FL 32925-3002

RONG-SONG JIH
DTRA/PMA
45045 AVIATION DRIVE
DULLES, VA 20166-7517

THOMAS JORDAN
MASS. INST. OF TECHNOLOGY
BLDG 54-918
CAMBRIDGE, MA 02139

LAWRENCE LIVERMORE NAT'L LAB
ATTN: TECHNICAL STAFF (PLS ROUTE)
PO BOX 808, MS L-208
LIVERMORE, CA 94551

LAWRENCE LIVERMORE NAT'L LAB
ATTN: TECHNICAL STAFF (PLS ROUTE)
PO BOX 808, MS L-205
LIVERMORE, CA 94551

LAWRENCE LIVERMORE NAT'L LAB
ATTN: TECHNICAL STAFF (PLS ROUTE)
PO BOX 808, MS L-200
LIVERMORE, CA 94551

THORNE LAY
UNIV. OF CALIFORNIA, SANTA CRUZ
EARTH SCIENCES DEPARTMENT
EARTH & MARINE SCIENCE BUILDING
SANTA CRUZ, CA 95064

ANATOLI L. LEVSHIN
DEPARTMENT OF PHYSICS
UNIVERSITY OF COLORADO
CAMPUS BOX 390
BOULDER, CO 80309-0309

JAMES LEWKOWICZ
WESTON GEOPHYSICAL CORP.
325 WEST MAIN STREET
NORTHBORO, MA 01532

LOS ALAMOS NATIONAL LABORATORY
ATTN: TECHNICAL STAFF (PLS ROUTE)
PO BOX 1663, MS D460
LOS ALAMOS, NM 87545

LOS ALAMOS NATIONAL LABORATORY
ATTN: TECHNICAL STAFF (PLS ROUTE)
PO BOX 1663, MS F665
LOS ALAMOS, NM 87545

LOS ALAMOS NATIONAL LABORATORY
ATTN: TECHNICAL STAFF (PLS ROUTE)
PO BOX 1663, MS C335
LOS ALAMOS, NM 87545

GARY MCCARTOR
SOUTHERN METHODIST UNIVERSITY
DEPARTMENT OF PHYSICS
DALLAS, TX 75275-0395

KEITH MCLAUGHLIN
CENTER FOR MONITORING RESEARCH
SAIC
1300 N. 17TH STREET, SUITE 1450
ARLINGTON, VA 22209

BRIAN MITCHELL
DEPT OF EARTH & ATMOSPHERIC SCIENCES
ST. LOUIS UNIVERSITY
3507 LACLEDE AVENUE
ST. LOUIS, MO 63103

RICHARD MORROW
USACDA/IVI
320 21ST STREET, N.W.
WASHINGTON DC 20451

JOHN MURPHY
MAXWELL TECHNOLOGIES
11800 SUNRISE VALLEY DRIVE
SUITE 1212
RESTON, VA 22091

JAMES NI
NEW MEXICO STATE UNIVERSITY
DEPARTMENT OF PHYSICS
LAS CRUCES, NM 88003

ROBERT NORTH
CENTER FOR MONITORING RESEARCH
1300 N. 17th STREET, SUITE 1450
ARLINGTON, VA 22209

OFFICE OF THE SECRETARY OF DEFENSE
DDR&E
WASHINGTON DC 20330

JOHN ORCUTT
INST. OF GEOPH. & PLANETARY PHYSICS
UNIV. OF CALIFORNIA, SAN DIEGO
LA JOLLA, CA 92093

PACIFIC NORTHWEST NAT'L LAB
ATTN: TECHNICAL STAFF (PLS ROUTE)
PO BOX 999, MS K5-12
RICHLAND, WA 99352

FRANK PILOTTE
HQ AFTAC/TT
1030 S. HIGHWAY A1A
PATRICK AFB, FL 32925-3002

KEITH PRIESTLEY
DEPARTMENT OF EARTH SCIENCES
UNIVERSITY OF CAMBRIDGE
MADINGLEY RISE, MADINGLEY ROAD
CAMBRIDGE, CB3 OEZ UK

JAY PULLI
BBN SYSTEMS AND TECHNOLOGIES, INC.
1300 NORTH 17TH STREET
ROSSLYN, VA 22209

DELAINE REITER
WESTON GEOPHYSICAL CORP.
73 STANDISH ROAD
WATERTOWN, MA 0472

PAUL RICHARDS
COLUMBIA UNIVERSITY
LAMONT-DOHERTY EARTH OBSERV.
PALISADES, NY 10964

MICHAEL RITZWOLLER
DEPARTMENT OF PHYSICS
UNIVERSITY OF COLORADO
CAMPUS BOX 390
BOULDER, CO 80309-0309

DAVID RUSSELL
HQ AFTAC/TTR
1030 SOUTH HIGHWAY A1A
PATRICK AFB, FL 32925-3002

CHANDAN SAIKIA
WOOODWARD-CLYDE FED. SERVICES
566 EL DORADO ST., SUITE 100
PASADENA, CA 91101-2560

SANDIA NATIONAL LABORATORY
ATTN: TECHNICAL STAFF (PLS ROUTE)
DEPT. 5704
MS 0979, PO BOX 5800
ALBUQUERQUE, NM 87185-0979

SANDIA NATIONAL LABORATORY
ATTN: TECHNICAL STAFF (PLS ROUTE)
DEPT. 9311
MS 1159, PO BOX 5800
ALBUQUERQUE, NM 87185-1159

SANDIA NATIONAL LABORATORY
ATTN: TECHNICAL STAFF (PLS ROUTE)
DEPT. 5736
MS 0655, PO BOX 5800
ALBUQUERQUE, NM 87185-0655

AVI SHAPIRA
SEISMOLOGY DIVISION
IPRG
P.O.B. 2286 NOLON 58122 ISRAEL

MATTHEW SIBOL
ENSCO, INC.
445 PINEDA CT.
MELBOURNE, FL 32940

JEFFRY STEVENS
MAXWELL TECHNOLOGIES
8888 BALBOA AVE.
SAN DIEGO, CA 92123-1506

TACTEC
BATTELLE MEMORIAL INSTITUTE
505 KING AVENUE
COLUMBUS, OH 43201 (FINAL REPORT)

LAWRENCE TURNBULL
ACIS
DCI/ACIS
WASHINGTON DC 20505

FRANK VERNON
UNIV. OF CALIFORNIA, SAN DIEGO
SCRIPPS INST. OF OCEANOGRAPHY
9500 GILMAN DRIVE
LA JOLLA, CA 92093-0225

RU SHAN WU
UNIV. OF CALIFORNIA, SANTA CRUZ
EARTH SCIENCES DEPT.
1156 HIGH STREET
SANTA CRUZ, CA 95064

JAMES E. ZOLLWEG
BOISE STATE UNIVERSITY
GEOSCIENCES DEPT.
1910 UNIVERSITY DRIVE
BOISE, ID 83725

SANDIA NATIONAL LABORATORY
ATTN: TECHNICAL STAFF (PLS ROUTE)
DEPT. 5704
MS 0655, PO BOX 5800
ALBUQUERQUE, NM 87185-0655

THOMAS SERENO JR.
SAIC
10260 CAMPUS POINT DRIVE
SAN DIEGO, CA 92121

ROBERT SHUMWAY
410 MRAK HALL
DIVISION OF STATISTICS
UNIVERSITY OF CALIFORNIA
DAVIS, CA 95616-8671

DAVID SIMPSON
IRIS
1200 NEW YORK AVE., NW
SUITE 800
WASHINGTON DC 20005

BRIAN SULLIVAN
BOSTON COLLEGE
INSITUTE FOR SPACE RESEARCH
140 COMMONWEALTH AVENUE
CHESTNUT HILL, MA 02167

NAFI TOKSOZ
EARTH RESOURCES LABORATORY
M.I.T.
42 CARLTON STREET, E34-440
CAMBRIDGE, MA 02142

GREG VAN DER VINK
IRIS
1200 NEW YORK AVE., NW
SUITE 800
WASHINGTON DC 20005

TERRY WALLACE
UNIVERSITY OF ARIZONA
DEPARTMENT OF GEOSCIENCES
BUILDING #77
TUCSON, AZ 85721

JIAKANG XIE
COLUMBIA UNIVERSITY
LAMONT DOHERTY EARTH OBSERV.
ROUTE 9W
PALISADES, NY 10964